# NAVAL POSTGRADUATE SCHOOL
## Monterey, California


# THESIS

## DEVELOPMENT OF A TEST MECHANISM FOR ANALYZING FORCE ATTRITION METHODOLOGIES WITHIN AGGREGATED COMBAT SIMULATIONS

by

Michael L. Shenk

June 1998

Thesis Advisor: Bard K. Mansager
Thesis Co-Advisor: James G. Taylor

# REPORT DOCUMENTATION PAGE

Form Approved OMB No. 0704-0188



| 1. AGENCY USE ONLY (*Leave blank*) | 2. REPORT DATE | 3. REPORT TYPE AND DATES COVERED |
|---|---|---|
| | June 1998 | Master's Thesis |

4. TITLE AND SUBTITLE DEVELOPMENT OF A TEST MECHANISM FOR ANALYZING FORCE ATTRITION METHODOLOGIES WITHIN AGGREGATED COMBAT SIMULATIONS

5. FUNDING NUMBERS

6. AUTHORS Shenk, Michael, L.

7. PERFORMING ORGANIZATION NAME(S) AND ADDRESS(ES)
Naval Postgraduate School
Monterey CA 93943-5000

8. PERFORMING ORGANIZATION REPORT NUMBER

9. SPONSORING/MONITORING AGENCY NAME(S) AND ADDRESS(ES)

10. SPONSORING/MONITORING AGENCY REPORT NUMBER

11. SUPPLEMENTARY NOTES The views expressed in this thesis are those of the author and do not reflect the official policy or position of the Department of Defense or the U.S. Government.

12a. DISTRIBUTION/AVAILABILITY STATEMENT
Approved for public release; distribution is unlimited.

12b. DISTRIBUTION CODE

13. ABSTRACT(*maximum 200 words*)

For aggregated combat simulation models, the methods for calculating force attrition must be based upon sound mathematical formulations and parameter estimations. With an inherent lack of representative combat data for modern warfare scenarios, one effective method for determining the required parameter estimates is to thoroughly analyze the output from a stochastically based high-resolution combat model. It is this development of attrition parameters process, which so profoundly influences the validity of aggregated simulations, that lacks any comprehensive documentation or mathematical justification within the modeling community. By examining the development and validity of these processes for parameter estimation, valid attrition calibration formulae can be determined and used within force attrition algorithms in order to more precisely and justifiably model aggregated combat operations. The establishment of a user-friendly test bed for examining this attrition rate development process will play a major role in solidifying the understanding, implementation, and validation of current and future process techniques.

| 14. SUBJECT TERMS | 15. NUMBER OF PAGES |
|---|---|
| Combat Modeling, JANUS, Simulation, Attrition, ATCAL | 125 |
| | 16. PRICE CODE |

| 17. SECURITY CLASSIFICATION OF REPORT | 18. SECURITY CLASSIFICATION OF THIS PAGE | 19. SECURITY CLASSIFICATION OF ABSTRACT | 20. LIMITATION OF ABSTRACT |
|---|---|---|---|
| Unclassified | Unclassified | Unclassified | UL |

NSN 7540-01-280-5500

Standard Form 298 (Rev. 2-89)
Prescribed by ANSI Std. 239-18 298-102

# DEVELOPMENT OF A TEST MECHANISM FOR ANALYZING FORCE ATTRITION METHODOLOGIES WITHIN AGGREGATED COMBAT SIMULATIONS

Michael L. Shenk
Captain(P), United States Army
B.S., Clarion University of Pennsylvania, 1988

Submitted in partial fulfillment of the
requirements for the degree of

**MASTER OF SCIENCE IN APPLIED MATHEMATICS**

from the

**NAVAL POSTGRADUATE SCHOOL**
**June 1998**

# ABSTRACT

For aggregated combat simulation models, the methods for calculating force attrition must be based upon sound mathematical formulations and parameter estimations. With an inherent lack of representative combat data for modern warfare scenarios, one effective method for determining the required parameter estimates is to thoroughly analyze the output from a stochastically based high-resolution combat model. It is this development of attrition parameters process, which so profoundly influences the validity of aggregated simulations, that lacks any comprehensive documentation or mathematical justification within the modeling community. By examining the development and validity of these processes for parameter estimation, valid attrition calibration formulae can be determined and used within force attrition algorithms in order to more precisely and justifiably model aggregated combat operations. The establishment of a user-friendly test bed for examining this attrition rate development process will play a major role in solidifying the understanding, implementation, and validation of current and future process techniques.

# TABLE OF CONTENTS

# LIST OF FIGURES

# LIST OF TABLES

# LIST OF ACRONYMS AND SYMBOLS

| | |
|---|---|
| 1 BCT/52 ID(M) | 1st Brigade Combat Team, 52d Infantry Division (Mechanized) |
| AA | Avenue of Approach |
| ATCAL | Attrition Calibration |
| AOAC | Armor Officer Advanced Course |
| BCT | Brigade Combat Team |
| BDE | Brigade |
| BLUEFOR | BLUE Forces Representing Friendly United States Forces |
| BN | Battalion |
| $C^3$ | Command, Control, and Communications |
| CAA | United States Army Concepts Analysis Agency |
| CAS | Close Air Support |
| CEM | Concepts Evaluation Model |
| CO | Company |
| COMAN | Combat Analysis Model developed by Gordon M. Clark |
| COSAGE | Combat Sample Generator |
| DoD | Department of Defense |
| DIV | Division |
| F\|F | Firer \| Firer Attrition Process |
| FT\|FT | Firer-Target \| Firer-Target Attrition Process |
| FPS | Firepower Score |
| FPI | Firepower Index |
| ITEM | Integrated Theater Engagement Model |

| | |
|---|---|
| JANUS | The United States Army's Premier High Resolution Simulation Software |
| JETS | The Janus Evaluator's Tool Set |
| km | kilometer |
| LOS | Line-of-Sight |
| MLE | Maximum Likelihood Estimation |
| MRR(-) | Soviet Style Motorized Rifle Regiment (less than full strength) |
| NIMA | National Imaging and Mapping Agency |
| NTC | United States Army's National Training Center |
| ODE | Ordinary Differential Equation |
| PLT | Platoon |
| REDFOR | RED Forces Representing Enemy Soviet Style Forces |
| RHS | Right-hand side |
| TACWAR | Tactical Warfare Model |
| TOW | Tube-Launched Optically-Tracked Wire-Guided Anti-Tank Missile |
| TRAC | Training Analysis Center |
| TRADOC | United States Army Training and Doctrine Command |
| VIC | Vector In Commander Model |

# I. INTRODUCTION

Combat modeling and simulation are important analysis tools available to military leaders and their supporting organizations which provide valuable insight into the study of military operations across the spectrum of conflict. Combat models are employed frequently to conduct investigative studies ranging from peacekeeping operations, which are relatively narrow in scope, to conventional maneuver warfare executed at the nation-state level. Commanders and their supporting planning staffs regularly seek the resulting output from the execution of combat models and simulations. Prior to the employment of man and machine into a hostile environment, tactical commanders have the capability to develop and assess their maneuver plans by use of combat models and simulations. Additionally, combat models and simulations are employed as training tools to rehearse command and control actions and operational procedures. While models and simulations are not in themselves predictors of the outcomes to military operations or plans, their ability to provide samples about possible outcomes is welcomed as a preliminary step prior to placing soldiers and equipment in harm's way. As such, the designers of these models constantly attempt to refine the representation of warfare to ensure the model is as accurate and believable as possible. It is important to note that many of the interactions and human factors which are inherent to a military force are difficult to replicate within a combat model or simulation. This fact must be recognized by those employing combat models and simulations for mission analysis and maneuver warfare planning.

One of the most important capabilities of combat models and simulations is their ability to calculate the attrition of personnel and systems of the engaged military forces. The prediction, analysis, and management of the attrition to personnel and equipment in combat are highly regarded as important tasks by military leaders and their staffs. And, as a result, the ability of combat models and simulations to capture attrition data is often a measurement of the model's usefulness. What follows is a

discussion of the development of attrition measurements within the context of combat models and simulations.

## A. BACKGROUND

Several important principles and concepts underlying the general class description of combat models and simulations are important to this development of attrition measurement. Combat models and simulations are generally subdivided into two categories, namely, high resolution and aggregated.

High resolution models are generally associated with smaller force compositions where each combatant and its associated weapon or maneuver system are explicitly represented in the simulation. The complicated combat processes are decomposed into highly detailed sequences of events and activities which are carried out explicitly within the simulation. This detailed sequence of events and activities lends itself to simulation time steps which are very short. It is not uncommon for high resolution models to represent time explicitly to the second, updating important information almost continuously. The goal of the high resolution model is to accurately model each combat process so that the simulation results are traceable using mathematical formulas and constructs. The characteristics associated with the entities represented in the simulation are related to their engineering specifications, physical performance data, and specified behavioral assumptions. The existence of this information link from the engineering level through the behavioral engagement assumptions is the single most important quality of a high resolution model. The capability of representing weapon systems and equipment at the engineering level enables an analyst to observe the possible effects of alternative system specifications on a pre-defined simulation. Individual system contributions to the overall simulation are effectively analyzed in high resolution models. Another feature associated with high resolution models is based upon their reliance on stochastic processes. Nearly all of the simulation algorithms above the engineering specification level are proba-

bilistic in nature. For example, consider a firing sequence. The firing system goes through several sequential actions prior to firing its weapon. These include target acquisition, target selection, firing, impact, and damage assessment. As these events are not of a fixed length in actual combat, their representation in simulation relies upon the use of highly probabilistic random variables. Calculations of this nature can lead to variance among independent trials of a given combat simulation. In order to obtain a reliable result with respect to the variance between stochastic calculations, the modeler must execute multiple runs of the same simulation to obtain the "averaged" result. One of the most significant limitations of high resolution models is their sheer size and complexity. The computer codes supporting high resolution models are highly complex and often quite large, stretching hardware and software to their limit. These computer codes are expensive to develop, run, and maintain. The complexity associated with representing each individual entity of the combat scenario at the engineering specification level causes another significant limitation of high resolution models, namely, force size. High resolution models are limited to relatively small forces. In ground maneuver terms, this limitation is normally associated with an upper bound of roughly 1000 combatants [Ref. 1] or on the order of battalion to brigade levels of combat.

Aggregated models, as the word implies, maintain varying levels of aggregation of the represented combatants. For example, an aggregated model may be capable of representing a group of riflemen with an associated consolidated firepower capability rather than the individual soldiers. The model then portrays the aggregated capabilities of the group of riflemen represented graphically as a single entity. Therefore, an entity representing a platoon of 30 riflemen would maintain the firepower and maneuver capabilities associated with the 30 individual weapons systems carried by the 30 riflemen. The extent of aggregation within combat models varies based upon the level of combat being modeled and the intended use of the model. The aggregation process is natural within the confines of military combat models because

of the hierarchical command structure inherent to maneuver forces. For example, the natural aggregation process associated with a generic ground maneuver organization is individual combatant, squad, platoon, company, battalion, brigade, division, corps, army, and theater. Depending upon the use of the model in question, one of these natural groupings (normally no lower than brigade) would mark the lowest level of representation within the simulation. Individual combatants and groups of combatants which are smaller than the basic size are not explicitly represented and the attributes associated with these combatants are lost to the simulation. Two important and distinctive aggregation patterns associated with models of this type are homogeneous and heterogeneous aggregation, and, the distinction between them is particularly important for attrition calculations. A homogeneous aggregation is one where the combat power of a unit with multiple and distinct combatants is combined into a single measure (or perhaps one for ground combat systems and a second for aircraft systems). Attrition computations are then based upon the relative power of the aggregated forces in battle subject to their combat power indices. Contrastingly, heterogeneous aggregation maintains a count of the number of surviving weapons systems of each distinct type. This method of aggregation allows the model to represent the different levels of effectiveness of a particular weapon system against its possible targets. This form of aggregation permits more accurate attrition modeling than the homogeneous model resulting in less information loss. As a result, the trend of most modern aggregated models is to follow a heterogeneous aggregation process.

As the size of the modeled entity increases in aggregated models, the precision to which they can be located on the simulated battlefield may be decreased. A modeled combatant may maintain a center location and a frontal width where the individual entities making up the aggregated unit are assumed to be somewhere in the unit region. Information about the individual entities within the aggregated unit may be kept in the form of averages, but any specificity about individual locations is lost. Thus, the first significant consequence of aggregation is the loss of individual char-

acteristics within aggregated units resulting in the use of their averaged properties where any inherent fluctuations have been smoothed. Analogous to the smoothing of individual variations is the handling of stochastic processes. Since aggregate models do not maintain a reference to what each individual combatant is doing at any given time, the complex probabilistic events found within high resolution models are replaced by averaged behaviors. The firing process described earlier (target acquisition, target selection, firing, impact, and damage assessment) within the context of high resolution models may be replaced in an aggregated model by computing the rate at which an average tank kills enemy tanks. This derived attrition rate implicitly defines each of the probabilistic processes described above with the stochastic variability suppressed. This fact leads to a descriptor generally associated with aggregated models, namely, deterministic. With the engineering specification level of detail and the probabilistic processes being suppressed within the aggregated model, many assumptions and scenario details get absorbed by the attrition rate number, which in itself is a highly variable entity.

Lastly, aggregated models lose the information associated with event sequencing since they do not keep track of individual actions. Thus, the precise times of critical events, such as target kills, are not available from aggregated model output. This results in the process averages being processed over relatively long periods of time (ranging from a few minutes to a 24 hour period) where the computation of total casualties occurs at the end of the time period. Again, careful consideration must be given to the attrition rate formulation in that there are at least two sides involved in the exchange of fires. Not all combatants on either side will survive to continue firing for the duration of the time period. For example, consider the following example and resulting conclusions:

> Extreme care must be taken to make the underlying assumptions clear in computing the rate data for such models. For example, a daily attrition rate for aircraft stationed at an airbase which is under attack may be inconsistent with the day's plan for those aircraft (they may be flying missions and thus

not on the ground when their base is attacked). A simulation which assesses attrition on an aggregated daily cycle cannot know whether the airbase attack coincided with aircraft on the ground, so an assumption must be made and figured into the attrition rate data.

Overall, then, the outstanding feature of aggregation in combat models is information loss. As a result, it is necessary to model combat processes using average behavior rather than individual behavior. Although values for the average process rates are generally computed outside the combat model, the complex nature of these rates demands that we devote considerable effort...to explaining their derivation. [Ref. 1]

An obvious question with regards to the given strengths and limitations of the described combat modeling and simulation approaches is why high resolution models are not extended to larger force sizes thus maintaining the admirable qualities of the high resolution definition. Unfortunately, the difficulty in making this extension lies within the limitations of computer hardware and software and the expansive execution time which would be associated with such large scale high resolution models. The sheer number and complexity of the individual combatants and their associated characteristics render the use of high resolution combat models for all combat simulations impractical and, in some cases, impossible. Additionally, the complex nature of command, control, and communications ($C^3$) between echeloned organizations is extremely difficult to model. The synergism and inherent lack of measurability of these traits would require many assumptions on the part of the modeler possibly reducing the degree of model believability. Thus, the resulting segregation of combat models into the high resolution and aggregated categories is a matter of necessity. It is important to note, however, that the two categories may not be entirely independent during their execution due to the aggregated models' possible reliance upon the outcomes of high resolution battle simulations for the derivation of attrition rate parameters. While there are several currently employed methods for calculating force attrition within aggregated models (to be presented in Chapter III), it remains true that the attrition of personnel, equipment, and supplies resulting from an engagement

must, at some point, be calculated within an aggregated simulation. The compromise which is of specific interest to this research is the algorithmic application of mathematical constructs to determine aggregated force attrition based upon high resolution results. For example, when an aggregated combat simulation reaches a point where two opposing forces engage in battle, the model may implicitly rely upon high resolution simulation results generated under similar environmental, force composition, and tactical conditions. The end result of the battle executed within the aggregated simulation would be new force levels for each of the engaged combatants derived primarily from a deterministic replay of a representative battle using the attrition rate coefficients derived from the high resolution simulation output. The intermediate process of estimating the attrition rates and replaying the battle mathematically is the conceptual link between high resolution and aggregated models. With the line dividing high resolution and aggregated models clear in definition only, both categories have an associated collection of applications which, when combined, adequately meet the needs of combat modeling and simulation.

## B. APPLICABILITY TO CURRENT PROCEDURES

In the United States Army and, moreover, the joint warfare community, one of the most frequently used high resolution models which provides the data necessary to generate the attrition rates for use in aggregated models is called the Combat Sample Generator (COSAGE) model. The COSAGE model is a (fairly) high resolution, stochastic model of division level ground combat which maintains a combatant resolution to friendly platoons and enemy companies. Within each maneuver unit, a heterogeneous list of individual weapon systems is arranged in combat formations, interactions between opposing weapon systems are computed, and individual weapons system survival is governed by the laws of probability. With respect to aircraft, close air support of the ground battle by tactical aircraft is resolved down to a detailed simulation of the flight of individual aircraft. At a point in the exe-

cution of an aggregated model where two opposing ground forces are positioned to engage in combat, the representative battle simulation is carried out as a mathematical algorithm based primarily upon the results of a high resolution simulation (COSAGE). The killer/victim results and the associated time series of individual attrition are analyzed and mathematically manipulated resulting in the development of attrition rate estimates for each individual weapon systems of each engaged force. This process is referred to as the attrition calibration (ATCAL) Phase I process and will be discussed in detail in Chapter IV. These derived attrition rates are then applied to a deterministic algorithm which, when executed or "replayed" with the force levels present in the aggregated model, calculates resulting force levels (by system). These updated quantities are then passed back to the aggregated model as it continues through its remaining processes. This secondary "replay" process is commonly referred to as ATCAL Phase II. Currently, several theater level models have the capacity to employ ATCAL Phases I and II. These include Tactical Warfare (TACWAR), Concepts Evaluation Model (CEM), and Integrated Theater Engagement Model (ITEM). Whether a particular theater level aggregated model employs the ATCAL algorithm as its method for calculating attrition is largely dependent upon the respective developers' and users' understanding of ATCAL's theoretical development and mathematical principles, which, in themselves, remain to be areas of active research. See [Ref. 2].

## C. PROBLEM STATEMENT

In order to support current and future investigations into the theoretical underpinnings and mathematical stability of the defining algorithms within ATCAL Phases I and II, researchers must have a "user friendly" method of obtaining and analyzing the necessary high resolution output data and validating the conjectures present in said algorithms. Additionally, as a starting point for the mathematical analysis, researchers must have a thorough understanding of the basic principles as-

sociated with the various methods of calculating force attrition. This capability for analysis and foundation for understanding do not exist outside of the United States Army Concepts Analysis Agency (CAA) and its proprietary implementation of the COSAGE model and ATCAL Phase I and II algorithms. The intent of this thesis is to develop the framework for a test bed capable of conducting detailed analysis of the attrition problem. By developing realistic high resolution ground combat simulations using the Janus simulation software, capturing the detailed killer/victim results and the associated time series of casualties, and applying these results to the study of the aggregated attrition problem, continued and specialized future research can be conducted in this discipline. Specifically, as an immediate result of this research, future inquires can be made into the validity and appropriateness of the currently accepted versions of the ATCAL Phases I and II algorithms aiding in the proper documentation of their conjectures and results. Moreover, with this vehicle for comparative analysis, efforts can expand to the development of alternative attrition algorithms to meet the needs of future aggregated modeling efforts.

## D. JANUS SIMULATION SOFTWARE

As the initial step in creating a functional test bed for the study of attrition, one must choose a vehicle to conduct the sample data base of high resolution simulations. Janus is the primary high resolution, interactive wargaming simulation software used by the United States Army for the modeling of brigade sized (and below) operations, and, its widespread availability within the military community, ease of use, and verified credibility make it an obvious choice for meeting the demands of this proposed analysis. Named for the two-faced Roman god who was the guardian of portals and the patron of beginnings and endings, Janus had its beginnings as a nuclear effects modeling simulation developed by the Lawrence Livermore National Laboratory of the University of California. [Ref. 3] Its applicability to tactical training and operations analysis quickly made it functional to the United States Army

Training and Doctrine Command (TRADOC), Training Analysis Center (TRAC). The current version is intended to satisfy both the combat development and training communities. Its versatility allows it to be used interactively as a man-in-the-loop simulation to replicate the effects of command and control on a realistic battlefield during the simulation as enemy activity develops. As an analysis tool, Janus can be used non-interactively thus reducing the variability introduced by human decision making during the simulation execution. Janus is a stochastic simulation in that the system determines the results of actions (like direct fire engagements) according to laws of probability. While the principle focus of Janus is on ground maneuver and artillery units, it also models weather and its effects, day and night visibility, engineer support, minefield employment and breaching, rotary and fixed wing aircraft, resupply operations, and chemical environments. The inherent flexibility of this simulation software allows its user to accurately model a multitude of combat scenarios.

## E. SCOPE AND LIMITATIONS

This research is unique in that there has been no other attempt to establish an independent capability for analyzing the aggregated attrition problem, specifically the ATCAL Phase I and II algorithms. This work will validate the capability of constructing a high resolution ground combat simulation in Janus for the purpose of deriving attrition rate parameters using the ATCAL Phase I and II algorithms. Additionally, there has been no attempt to configure the Janus output data to conform to the requirements of the current ATCAL Phase I and II algorithms (currently existing in the FORTRAN computer language). This procedure and the transformation of the output data is practical only within the confines of analysis and algorithm validation because of the time expenditure required to develop the ground combat scenario in Janus and the nonexistence of automated software to link the Janus killer/victim results to current aggregated models. With initial efforts confined to the manual compilation of Janus output data and the explicit formulation and calculation of basic

mathematical models, this research could be expanded to focus on the compatibility and automation of the data linkage between Janus the current and/or future ATCAL computer codes. However, this is not the focus of this thesis. And, as only one specific ground combat simulation will be presented as part of this thesis, follow-on work is applicable in the development of additional scenarios with varying mission objectives, force definitions, environmental conditions, and terrain selections in order to generalize results otherwise limited to specific simulation parameters. A robust collection of simulations would be required to properly validate the conjectures presented in the problem statement. As such, the results presented in this work relate only to the specific scenario and situations modeled and should not be considered to be the final solution.

# II. THE SIMULATION SCENARIO

In order to generate the required high resolution output data with Janus for the development of attrition rate numbers using the ATCAL Phase I and II algorithms (analogous to the process described in Chapter I, Section B), the author has chosen to simulate a heavy brigade combat team (BCT) combat scenario. The typical heavy BCT includes a heterogeneous mix of direct fire, indirect fire, and supporting maneuver systems. Generically, the force would include tanks, armored personnel carriers, artillery systems, air defense artillery systems, engineering equipment, wheeled vehicles, air assets, and obstacles. The BCT is the preferred level of combatant organization for this study because of the described combined arms composition and the ability to portray this force in Janus. As a high resolution model, Janus can effectively support a force type of this size and capture the detailed results of all direct and indirect fire engagements. With these results, the attrition rate estimation process (ATCAL Phase I) and the deterministic battle replay (ATCAL Phase II) can be conducted.

The tactical scenario chosen for this combat simulation is one of practical relevance. As this research focuses primarily on the modeling of ground combat as part of an overlying larger tactical operation, the author has chosen to simulate the mechanized task force operations in desert environmental conditions as a baseline scenario. As the Janus simulation package can be an interactive training tool when employed as a man-in-the-loop simulation, it is often used by TRADOC at the United States Army's combat arms training centers. Specifically, the Armor Officer Advanced Course (AOAC) located at the Unites States Army Armor Center, Fort Knox, Kentucky, employs Janus as a tool to train and evaluate the mission planning and tactical decision making skills of its officer students. With a specified mission of training the current and future leaders of the United States maneuver warfare organizations, AOAC and its focus on modern ground maneuver tactics, techniques, and

procedures provide an excellent simulation opportunity for this research. The Janus simulation used during this research was executed by AOAC Class 97-3 at the Fort Knox Brigade Battle Simulation Center. [Ref. 4] And, the simulation is available for review through coordination with Professor Bard K. Mansager, Department of Mathematics, Naval Postgraduate School. The stochastic nature of the simulation is defined not only by the probabilistic events which occur as a function of the intrinsic algorithms, but also by the human factors associated with the particular officer students who executed the simulation. If multiple runs of this scenario were executed, each would produce different results based upon these stochastic processes.

## A. MECHANICS OF THE SIMULATION

At the highest level of organization, Janus allows the definition of six combatant *sides* where each *side* could represents an autonomous force. Under each *side*, forces can be further organized into *task forces* where modeled weapons and maneuver systems can be organized and manipulated in groupings that mirror their real life task organization. After the defined combatants are organized into *task forces*, one or more of these *task forces* are output to a specific computer workstation for user control. Janus permits up to 24 computer workstations to be in use during a simulation. The 24 workstations are divided into *side* 1 through *side* 6 terminals based upon the number of users assigned to manipulate the respective *sides* and *task forces*. [Ref. 5] The simulation used for this research makes use of *sides* 1 and 2 and will hereafter be referred to as BLUE and RED, respectively. This assignment represents the roles of the combatants during the simulation. In this simulation, BLUE represents the friendly Unites States forces being controlled by the AOAC 97-3 student officers and RED represents a Soviet-style enemy forces being controlled by designated opposing force personnel.

## 1. BLUE Force Composition and Organization

The BLUE force (BLUEFOR) is made up of the United States maneuver and weapons systems appearing in Appendix A, Table XIII on page 64; and, when organized for combat, these systems represents a heavy BCT. The BLUEFOR is considered to be "balanced" in terms of its armor to mechanized infantry ratio. As an integrated combined arms fighting force, the BLUEFOR systems are organized into a typical BCT hierarchical command and control structure as detailed by Table I. For the purposes of the AOAC student officers who executed the Janus simulation, this fictitious force was designated as the 1st Brigade Combat Team (1 BCT).

| Unit Description | Major Systems |
|---|---|
| 4 Direct Fire Maneuver Battalions | M1A1, M2 |
| 2 Indirect Fire Artillery Battalions | M109A6 |
| 1 Air Defense Artillery Company | BSFV |
| 1 Chemical Support Company | IF TRU |
| 1 Engineer Support Battalion | AVLM |
| 1 Logistics Support Battalion | IF TRU |
| 1 Tactical Air Control Party | A10 (6) |

Table I. BLUEFOR Task Organization for AOAC 97-3 Janus Simulation [Ref. 6]

## 2. RED Force Composition and Organization

The RED force (REDFOR) is made up of Soviet style equipment listed in Appendix A, Table XII on page 63; and, when organized for combat, it represents a less than full strength Soviet style motorized rifle regiment [MRR(-)]. Note the greater than three to one ratio of mechanized infantry to armor, implying that the REDFOR is better equipped for mechanized infantry operations than tank warfare. Additionally, the REDFOR has a significant number of indirect fire artillery systems at its disposal. The defensive REDFOR MRR(-) is organized within the hierarchical command and control structure detailed by Table II. For the purposes of the AOAC

student officers who executed the Janus simulation, this fictitious enemy force was designated as the 168th MRR(-).

| Unit Description | Major Systems |
|---|---|
| 2 Direct Fire Maneuver Battalions | BMP |
| 1 Direct Fire Tank Battalion | T80 |
| 4 Indirect Fire Artillery Battalions | 2S1, 2S5, BM-21 |
| 1 Air Defense Artillery Company | SA7, ZSU-23 |
| 1 Engineer Support Company | MTK-LI |
| 1 Logistics Support Company | IF TRU |
| 1 Helicopter Company | HIND (6) |

Table II. REDFOR Task Organization for AOAC 97-3 Janus Simulation [Ref. 6]

## B. TERRAIN REPRESENTATION

The Janus simulation uses digitized terrain developed by the United States National Imaging and Mapping Agency (NIMA). The terrain selected for this simulation is located within the United States Army's National Training Center (NTC) near Barstow, California, covering a 100 $km^2$ area with actual military grid coordinate locations defined by the corner points NK800400, NK790400, NK790390, and NK800390. The terrain is displayed in Janus similar to that used by military personnel during actual training and combat operations. It includes contour lines (elevation information), roads, rivers, vegetation, and urban areas. The visibility issues associated with terrain elevation and visual obstructions are realistically portrayed in Janus. These modeled attributes will degrade (or enhance) a combatant's line-of-sight (LOS) and movement. The modeled vehicles and equipment must maneuver under the conditions represented by the digital terrain and its overlying natural and man-made features. For example, only those vehicles with a "swim" capability for crossing water obstacles are permitted to do so without employing bridging assets; and, when executed, the vehicles will proceed at a reduced movement rate.

The environmental conditions and time of battle are also controlled in Janus. The user can specify environmental conditions including temperature, cloud conditions, and air characteristics affecting smoke propagation. Weather and its effects influence the visibility and movement of the modeled combatants. The start time can be set in order to execute the combat simulation at a particular time of day. This accounts for simulating day and night operations which also affect visibility and movement attributes. The environmental conditions used during this simulation were summer, desert with 14 kilometers (km) visibility, and a 0800 start time. Since Janus accurately models the BLUEFOR and REDFOR weapons systems as a function of each system's capabilities as defined in the database, users must consider all military aspects of employing their forces just as they would in actual combat. Invariably, Janus will reveal the weaknesses associated with poor planning and reward those who have tactically sound plans. As the combat scenario for this research was executed by students of the mounted warfare profession, the author assumes the employment of tactically sound techniques, procedures, and plans.

## C. SCENARIO EXECUTION SUMMARY

The initial dispositions of BLUEFOR and REDFOR are depicted in Appendix A, Figures 1 and 2 on pages 65 and 67, respectively. The BLUEFOR mission is to attack in zone to destroy or cause the withdrawal of the 168th MRR(-) security zone forces who are controlling the key terrain in and around grid coordinate NK620130 (Avawatz Mountain Passes) [Ref. 6]. The BLUEFOR executes a supporting attack in the north followed by a main attack in the south. The REDFOR conducts a defensive operation with an objective of stopping the penetration of the BLUEFOR and defending the significant terrain as mentioned above [Ref. 6]. The REDFOR executes a layered defense with two distinct defensive belts supported by deliberate minefields, obstacles, and barriers.

At the onset, the BLUEFOR is positioned to conduct offensive operations using two distinct avenues of approach (AA). For the purpose of this research, the northern and southern AAs will be named AA North and AA South, respectively. The main effort of the BLUEFOR attacks along AA South with the supporting attack along AA North. As a matter of mounted warfare tactics, the BLUEFOR leads with reconnaissance assets in order to locate and direct fires upon the REDFOR's defensive assets. Following closely behind are the BLUEFOR's initial maneuver and engineering assets. This battlefield organization will support direct fire engagements with the REDFOR upon their detection by the BLUEFOR reconnaissance elements. The BLUEFOR engineering elements are positioned forward to facilitate the clearing of obstacles and breaching of REDFOR minefields. Next in the BLUEFOR order of battle is the bulk of the fighting forces primarily consisting of tanks and armored personnel carriers. The indirect fire artillery assets follow in the BLUEFOR combat formation. They are positioned in an attempt to be within range of the REDFOR while maintaining reasonable security from REDFOR counter-artillery operations. Finally, the support oriented vehicles and equipment make up the rear of the attacking BLUEFOR. Positioned well to the rear and in support of the BLUEFOR, six A-10 close air support (CAS) aircraft are available to be employed as a coordinated part of the attack.

The REDFOR, while maintaining a layered defense supported by maneuver obstacles and minefields, also maintains a counterattack capability with reserve forces located to the rear of their main defensive area. These combatants can be employed to reinforce weakened defensive areas or to counter a penetrating attack made by the BLUEFOR. As detailed by Table II, the REDFOR is primarily a mechanized force consisting of armored personnel carriers. As such, the REDFOR's tanks are employed judiciously and in positions where they can have the most significant effect on the attacking BLUEFOR. One of the most significant capabilities of the REDFOR is found in the number of supporting indirect fire artillery assets. The REDFOR maintains

both a close and long range indirect fire capability while keeping the majority of its artillery assets outside of the maximum range of the BLUEFOR's artillery units. The REDFOR emphasizes the use of its indirect fire systems and their associated radar systems to locate and conduct counter-battery fire against the BLUEFOR. As the simulation progresses, the REDFOR attempts to halt the advance of the attacking BLUEFOR.

## 1. Execution Summary: 0 to 30 Minutes

The BLUEFOR begins offensive operations by employing its leading reconnaissance assets in AA North. Shortly thereafter, the BLUEFOR and REDFOR make contact with each other and exchange direct fires. At approximately 11 minutes, the REDFOR long range artillery assets fire special munitions placing two area minefields each containing 480 anti-armor mines to thwart the advance of the attacking BLUEFOR in the north. As of yet, the BLUEFOR attacking along AA South have not made contact with the REDFOR defensive positions in that area. During and immediately following the BLUEFOR's minefield breaching operations in the north, a heated direct fire battle takes place. Both sides employ their indirect fire artillery assets as their reconnaissance assets fix each other's locations on the battlefield. With 28 BLUEFOR and 9 REDFOR combatants killed during this 15 minute localized battle, the BLUEFOR attacking along AA North are able to overwhelm the REDFOR defensive forces and break through the first defensive line in the north. Shortly thereafter, at approximately 27 minutes, the REDFOR long range artillery assets reposition to alternate firing positions for security purposes.

See Appendix A, Figure 3 on page 69 for a pictorial representation of the battlefield at the beginning of the scenario. Table III below details the force attrition at the completion of the 0 to 30 minute time period. See Appendix A, Figure 4 on page 71 for a pictorial representation of the battlefield at 30 minutes.

| | BLUEFOR Losses | REDFOR Losses |
|---|---|---|
| Direct Fire | 34 | 10 |
| Indirect Fire | 7 | 4 |
| Minefields | 4 | 0 |
| **Cumulative Losses at 30 Minutes** | 45 | 14 |

Table III. Force Losses for AOAC 97-3 Janus Simulation at 30 Minutes

## 2. Execution Summary: 31 to 60 Minutes

The BLUEFOR, who met with success in the north, proceed east-northeast on a high speed AA and are met with little resistance from the REDFOR. At approximately 40 minutes, the attacking BLUEFOR moving along AA South come in contact with the first layer of REDFOR defenders in the south. The majority of the BLUEFOR following the two attacks begin movement north-northeast to take advantage of the successful penetration of the REDFOR's northern defenses. The BLUEFOR in contact in the south encounter and begin breaching operations on three linear minefields positioned in front of the REDFOR. As BLUEFOR reconnaissance forces identify REDFOR targets to their front they direct indirect artillery fires against them resulting in only marginal success. At approximately 45 minutes, the remainder of the REDFOR's defending forces in the first defensive layer engage the attacking BLUEFOR from AA South. The REDFOR defense in the south is much more formidable than that which was found in the north. The BLUEFOR has some difficulty identifying penetration points through the REDFOR's defenses. The BLUEFOR suffers a large number of casualties during this battle. The main body of the BLUEFOR compresses into a more compact movement formation and increases its movement rate.

Table IV details the force attrition at the completion of the 31 to 60 minute time period. See Appendix A, Figure 5 on page 73 for a pictorial representation of the battlefield at 60 minutes.

| | BLUEFOR Losses | REDFOR Losses |
|---|---|---|
| Direct Fire | 51 | 14 |
| Indirect Fire | 9 | 4 |
| Minefields | 4 | 0 |
| **Cumulative Losses at 60 Minutes** | 64 | 18 |

Table IV. Force Losses for AOAC 97-3 Janus Simulation at 60 Minutes

## 3. Execution Summary: 61 to 90 Minutes

By 65 minutes, the BLUEFOR attacking in AA South are massed at the forward edge of the linear minefields and conducting passage through the cleared lanes. At the same time, six A-10 CAS aircraft enter an aerial holding area for possible employment against the REDFOR in the first defensive belt. The REDFOR has a small ambush or counter-attack force made up of two tanks and two armored personnel carriers positioned at the extreme south-southeast of its first defensive layer in order to block the advancing BLUEFOR from using a high speed AA. However, the overwhelming BLUEFOR combat power moving through this area quickly engages and destroys this team. At this point, the BLUEFOR begins to reorient its forward movement to the north to take advantage of the previous success there. At approximately 83 minutes, the BLUEFOR attacking to the north-northeast along AA North make contact with the second layer of REDFOR defenses. The BLUEFOR begins an indirect artillery barrage against these REDFOR.

Table V details the force attrition at the completion of the 61 to 90 minute time period. See Appendix A, Figure 6 on page 75 for a pictorial representation of the battlefield at 90 minutes.

| | BLUEFOR Losses | REDFOR Losses |
|---|---|---|
| Direct Fire | 65 | 25 |
| Indirect Fire | 10 | 5 |
| Minefields | 7 | 0 |
| **Cumulative Losses at 90 Minutes** | 82 | 30 |

Table V. Force Losses for AOAC 97-3 Janus Simulation at 90 Minutes

## 4. Execution Summary: 91 to 120 Minutes

At approximately 93 minutes, the six A-10 CAS aircraft depart the aerial holding area to attack the second layer of the REDFOR defenses from the southeast to the northwest. Shortly thereafter, at 100 minutes, two REDFOR radar controlled anti-aircraft systems engage and destroy three A-10 CAS aircraft. The remaining aircraft adjust their course and continue their attack on the defending REDFOR combatants. Prior to their egress, the remaining three A-10 CAS aircraft are destroyed by REDFOR shoulder-fired anti-aircraft missiles located in the northeast. By 105 minutes, the main BLUEFOR attacking elements clear the linear minefields and being their movement north-northeast along the high speed AA. At 116 minutes, these attacking BLUEFOR make contact and exchange initial fires with the remainder of the REDFOR's second layer defensive forces in the central and southern portion of the maneuver area. Heavy exchanges of artillery occur during the development of this high intensity battle.

Table VI details the force attrition at the completion of the 91 to 120 minute time period. See Appendix A, Figure 7 on page 77 for a pictorial representation of the battlefield at 120 minutes.

| | BLUEFOR Losses | REDFOR Losses |
|---|---|---|
| Direct Fire | 92 | 35 |
| Indirect Fire | 24 | 9 |
| Minefields | 12 | 0 |
| **Cumulative Losses at 120 Minutes** | 128 | 44 |

Table VI. Force Losses for AOAC 97-3 Janus Simulation at 120 Minutes

## 5. Execution Summary: 121 to 150 Minutes

During the battle within the second layer of the REDFOR defense, six additional A-10 CAS aircraft are called forward from their staging area to attack the defending forces. The majority of the six aircraft are highly successful until their destruction at 131 minutes by radar controlled anti-aircraft fires. Heavy exchanges of

direct fires continue to occur and the attacking BLUEFOR divides its formation into two distinct attacks, one to the north-northwest and another along the high speed AA to the east-northeast.

Table VII details the force attrition at the completion of the 121 to 150 minute time period. See Appendix A, Figure 8 on page 79 for a pictorial representation of the battlefield at 150 minutes.

| | BLUEFOR Losses | REDFOR Losses |
|---|---|---|
| Direct Fire | 139 | 49 |
| Indirect Fire | 32 | 9 |
| Minefields | 22 | 0 |
| **Cumulative Losses at 150 Minutes** | 193 | 58 |

Table VII. Force Losses for AOAC 97-3 Janus Simulation at 150 Minutes

## 6. Execution Summary: 151 to 180 Minutes

The BLUEFOR attack to the north-northwest meets with a tank heavy REDFOR defensive element including some reserve forces coming from behind the second defensive layer. The BLUEFOR reacts by passing additional tank assets through to the front of its formation in an attempt to counter the REDFOR tank threat with like firepower. At 158 minutes, the BLUEFOR in the northwest directs indirect artillery fires against the REDFOR with little effect. At 165 minutes, the main body of the BLUEFOR which was following the lead attacking forces moves farther forward to concentrate fires. The direct fire battle in the north-northwest becomes a battle of attrition with the BLUEFOR maintaining numerical superiority. However, this translated into a target rich environment for the REDFOR. A successful penetration of the defense occurs and BLUEFOR continues their northwestern movement past the REDFOR's second layer of defense. As the breakthrough occurs, the REDFOR in the south take advantage of the flanking shot opportunities against the passing BLUEFOR and are rewarded with a large number of kills. This time period

is marked by the BLUEFOR's largest number of direct fire losses as compared to any other 30 minute time period.

Table VIII details the force attrition at the completion of the 151 to 180 minute time period. See Appendix A, Figure 9 on page 81 for a pictorial representation of the battlefield at 180 minutes.

| | BLUEFOR Losses | REDFOR Losses |
|---|---|---|
| Direct Fire | 254 | 63 |
| Indirect Fire | 44 | 9 |
| Minefields | 27 | 0 |
| **Cumulative Losses at 180 Minutes** | 325 | 72 |

Table VIII. Force Losses for AOAC 97-3 Janus Simulation at 180 Minutes

## 7. Execution Summary: 181 to 211 Minutes

The BLUEFOR divides into two relatively equally sized formations with one attacking north-northeast and the second, south of the first, attacking along the high speed AA to the northeast. At 188 minutes, the REDFOR commits its reserves in the north to counter the BLUEFOR attack in that sector. After some success, the numerically superior BLUEFOR destroys the employed reserves. At 198 minutes, the BLUEFOR in the south completely clears the second defensive layer and all of its associated minefields. At 206 minutes, the REDFOR commits addition reserve forces against the BLUEFOR attacking in the south along the high speed AA in an attempt to thwart the advance. At 211 minutes, the combat simulation is terminated simulating the achievement of one or more of the BLUEFOR commander's ending conditions. Battle termination standards may include attrition to a specified force level, attrition to a specified number of remaining maneuver systems, and/or the accomplishment of stated objectives. This particular combat simulation was undoubtedly stopped due to a self-imposed time constraint as the simulation was executed by and for the benefit of AOAC Class 97-3.

Table IX details the force attrition at the completion of the simulation. See Appendix A, Figure 10 on page 83 for a pictorial representation of the battlefield at the completion of the simulation.

| | BLUEFOR Losses | REDFOR Losses |
|---|---|---|
| Direct Fire | 270 | 79 |
| Indirect Fire | 45 | 9 |
| Minefields | 29 | 0 |
| **Cumulative Losses at Completion Minutes** | 344 | 88 |

Table IX. Force Losses for AOAC 97-3 Janus Simulation at Completion

## D. UTILIZATION OF THE SIMULATION OUTPUT

One of the most advantageous properties of the Janus simulation software is its ability to capture information about the execution of the combat scenario. The force loss totals detailed in the tables above are just samples of the information available to the Janus analyst. The Janus post execution output files which are important to the attrition rate analysis of this research include the direct fire report, coroner's report, killer/victim scoreboard, and the artillery impacts report. While several other reports are available, these four reports will provide the time series of casualties data required for the development of attrition rate estimates applicable to the ATCAL Phase I algorithm. With the required simulation output data in hand, what remains to be developed are the mathematical constructs which serve as the basis for the ATCAL Phase I and II algorithms.

# III. ATTRITION METHODOLOGIES FOR AGGREGATED MODELS

## A. BACKGROUND

Prior to any detailed analysis of the attrition rate estimate process as it applies to the ATCAL Phase I and II algorithms (the primary goal of this research), it is important to establish a foundation with respect to the various methods for calculating attrition and determining the outcomes of battles within aggregated simulations. In general, nearly all attrition computation methodologies can be categorized by two techniques: the Anderson (Force-Ratio [FR]) model and some type of Lanchester-type model. Integral to the second attrition approach are the Bonder-Ferrell method and the Combat Analysis (COMAN) maximum likelihood estimation (MLE) method for determining attrition coefficients for use in Lanchester-type equations (of which variants are used in the ATCAL algorithms). Although the COMAN MLE approach is not specifically used within any current models, its applicability to the attrition modeling cannot be overstated. Each of these distinct attrition methodologies maintains a relevance to modern aggregated modeling. For example (although not all-inclusive), the Anderson (FR) method is one of the two options for assessing attrition in TACWAR 4.1, the Bonder-Ferrell method is employed within the United States Army's Vector In Commander (VIC) model, and the ATCAL methodology is used in CEM and ITEM. (TACWAR also has an option to use the ATCAL attrition methodology rather than FR.) One of the most interesting facts of this research is that ATCAL uses none of the attrition methodologies (explicitly) as they are described below. Rather, ATCAL uses an *ad hoc* method for attrition rate estimation. This is truly one of the mysteries of ATCAL for which this research attempts to establish the vehicle for further analysis.

## B. THE ANDERSON (FR) BASED ATTRITION MODEL

In this theory, a heterogeneous force (its overall strength) can be described by one scalar value representing the consolidated individual systems' contributions to the force as a whole. Each system maintains an assigned value (score) relative to some common weighting criteria. Summing over all systems multiplied by their respective value (score) results in the generation of an overall firepower index (FPI) for the force being represented. As this FPI is a single scalar value, the resulting process is characterized as a homogeneous force ratio attrition model. The explicit representation of the heterogeneous force is replaced by this single scalar measure of combat power. This strategy can be expressed mathematically for a hypothetical force, $X$, as shown below in Equation III.1.

$$\text{FPI}_X = \sum_{i=1}^{m} S_i^X X_i \qquad \text{(Firepower Score)} \qquad \text{(III.1)}$$

$i$ = integer index each representing a unique weapon system type, total of $m$

$S_i^X$ = value (score) of one weapon system of type $i$

$X_i$ = number of weapon system of type $i$

Supposing that the FPI of two opposing forces ($X$ and $Y$) are represented by $\text{FPI}_X$ and $\text{FPI}_Y$, respectively, then the force ratio, $\text{FR}_{XY} = \dfrac{\text{FPI}_X}{\text{FPI}_Y}$, gives a measure of relative combat power at the instant at which the values are calculated. The $\text{FR}_{XY}$ may be used to determine force missions, unit postures, casualty computations, and mission success. Specifically, the $\text{FR}_{XY}$ can be indexed against personnel loss curves to determine attrition to modeled forces. The loss curves employed in this process are generally derived from the results of historical battles. This fact is considered to be one the inherent strengths of the Anderson (FR) method. On the other hand, one of the perceived weaknesses of this method is associated with the determination of the individual weapon system values (scores) as discussed below.

## 1. Determination of Weapon System Value

There is no general agreement in the modeling community on how to determine the individual weapon system values (scores), $S_i^X$. The fundamental methods for determining firepower score values include analysts' perception of combat value (the naive estimate), historical combat performance, measures of weapon firepower and support platform characteristics, and, finally, measures of what a weapon can kill. This last method attempts to compute the value (score) for a weapon as being proportional to the rate at which it destroys the value of opposing enemy systems, and, as such, becomes a circularly defined problem. Moreover, this approach's dependence on the "rate" at which weapons destroy opposing weapons in battle infers the reliance upon assumed or derived non-negative scalar attrition rates (one for each weapon system firing at every opposing weapon system for both forces) which account for the highly detailed engagement process described in Chapter I. The mathematics of this method, called the AntiPotential-Potential (APP) method, amounts to solving for the individual weapon system scores through a linear system of equations (in matrix form) as detailed below by Equations III.2 and III.3. The solutions to these equations are found by solving an equivalent system of eigenvalue problems [Ref. 1], for which the development is beyond the scope of this discussion. However, as a practical example, Appendix B details the application of the Anderson (FR) method and the subordinate APP process to hypothetical high resolution output data representative of the AOAC 97-3 Janus simulation described in Chapter II. The calculations are sampled from the heterogeneous battle between selected BLUEFOR and REDFOR weapon systems. Note that this computational excursion does not account for every weapon system modeled in the Janus Simulation in an attempt to keep the associated eigenvalue problem numerically solvable in closed form without the aid of automated software.

$$C_X S_i^X = \sum_{j=1}^{n} K_{ij} S_j^Y \tag{III.2}$$

$$C_Y S_j^Y = \sum_{i=1}^{m} L_{ji} S_i^X \tag{III.3}$$

Force $X$ = $\{x_1, x_2, x_3, \ldots, x_m\}$ m distinct weapon systems

Force $Y$ = $\{y_1, y_2, y_3, \ldots, y_n\}$ n distinct weapon systems

$S_i^X$ = value of one type $i$ system in $X$ force

$S_j^Y$ = value of one type $j$ system in $Y$ force

$K_{ij}$ = matrix of rates at which one $X_i$ system kills $Y_j$systems

$L_{ji}$ = matrix of rates at which one $Y_j$ system kills $X_i$systems

$C_X$ = proportionality constant

$C_Y$ = proportionality constant

## 2. Advantages and Disadvantages

The use of historical data, both in the generation of personnel and equipment loss curves and in the determination of weapon system values, generates a certain level of model believability and personal comfortableness with the Anderson (FR) method of attrition. Moreover, aggregated simulations using this method are credited with reproducing comparable results to the recorded outcomes of actual battles. This trait is often considered important when attempting to validate and verify a model's usefulness. The desire to extend these result to the modeling of future battles is a task which generates a considerable amount of discussion. With respect to determining weapon system values (scores), the APP method and its associated eigenvalue problem are an attractive procedure for calculating homogeneous force values and resulting force ratios for use in aggregated models because of their mathematical ease of computation (regardless of their appropriateness).

Conversely, there are a significant number of limitations inherent to this procedure. A major criticism of this method is that the APP scoring method may be inconsistent with the personnel loss curves which are generally based upon historical data. Additionally, since Equation III.1 is additive across weapon systems, there is no ability to represent the interactions among complementary weapons on the battlefield. This is an especially serious shortcoming considering the nature of the current battlefield and the synergies of modern weapon systems. One must exercise caution when conducting comparative assessments of force mix or force balance since the scalars $FPI_X$ and $FPI_Y$ do not discriminate between balanced and unbalanced forces (in terms of size). An $FPI_X = 100$ and an $FPI_Y = 100$ are equal forces using this method regardless of the number of systems represented or their respective values. The reader will also note that Equation III.1 is linear in the number of weapons $X_i$ of each weapon type $i$. Therefore, a model employing the Anderson (FR) method cannot be expected to effectively answer specific questions about the contributions of individual weapons. For example, the ramifications of an unmanageably large number of a specific weapon may be intuitively obvious, but, the FR model will linearly increase the overall FPI without regard to practicality. It is the opinion of the author that the overwhelmingly mysterious characteristic of the Anderson (FR) method lies within the development of the individual weapon system values (scores). The reader may have surmised that in order to apply the Anderson (FR) method, the analyst is forced to arbitrarily assume values (scores) for each of the modeled weapon systems or to rely upon the killer/victim results of high resolution simulation to develop the attrition rates necessary to employ the APP method of solving for weapon system values (scores). Associated with using the high resolution simulation results to derive the kill rates within the APP method for increased believability, the reader should be aware of some of the inherent weaknesses which plague the APP eigenvalue problem. The score values derived from the eigenvalue problem are extremely dependent upon scenario characteristics and the number of weapons systems which translate into tar-

get engagement opportunities. Changes to the attrition rates (the key elements to the APP method) will typically cause all weapon system score values to change for both forces in ways that are hard to describe or justify. Consider another author's evaluation of the APP method of determining weapon system values:

> The eigenvector score values sometimes change in ways that are hard to explain and that have been called paradoxical by some. For example, a shift in fire distribution designed to increase the kill rates of a higher value enemy target can sometimes reduce the total value index of the firing force. Whether this is, in fact, paradoxical depends on how deeply the relationships are followed. If there are few of the high value target, then shifting fire away from a lower value but more numerous enemy system might very well result in a lower total value being killed by the firing force.
>
> Other anomalies, however, are harder to explain. The numeric values of the scores are sometimes oversensitive to small changes in the input kill rate matrices... [Ref. 1]

It is with this knowledge that the analyst is drawn to developing similar methodologies using nonlinear value equations, a formidable excursion which is beyond the scope of this research.

## 3. Typical Implementation of the Anderson (FR) Method

A generic aggregated combat model, like TACWAR may employ the Anderson (FR) method for attrition calculations in the following way. Assume that a hypothetical model represents opposing forces down to the division level of organization. The model would compute attrition for the divisions in a combat sector with an update cycle equal to the overall time cycle of the model, possible every 12 or 24 hours. Prior to the calculation of attrition, the simulation schedules several events to update the forces. These tasks may include movement of forces into and out of the combat sectors, allocation of reinforcements, determination of which force is the attacker for the cycle, determination of the defender's posture for the cycle, and computation of the results of any scheduled air battles for the cycle. At a point during the execution of a generic aggregated combat simulation where the conditions are met for two

opposing divisions to engage in battle, the Anderson (FR) method would be invoked to determine the respective forces' FPIs. In a simplified sense, the resultant $FR_{XY}$ determines the outcome of the battle with respect to losses. After computing (mostly estimating) the parameters required for the Anderson (FR) and subordinate APP calculations, the resulting $FR_{XY}$ values are indexed against the appropriate personnel casualty curve to determine overall attrition levels. (Unfortunately, indexing the $FR_{XY}$ against the casualty rate and equipment loss curves may not be consistent due to differing computational methods. The $FR_{XY}$ is derived using a linear model including the APP process, while the casualty rate and equipment loss curves may have been derived nonlinearly from historical data.) During each time cycle of the simulation (possibly 12 or 24 hours), the APP eigenvalue problem must be recursively solved to determine the updated weapon system scores and the resulting forces' FPIs due to their dependence on the number of individual weapon systems remaining. This entire process is simply repeated as the simulation continues through additional time cycles.

## C. LANCHESTER-TYPE DIFFERENTIAL ATTRITION MODELS

Prior to discussing the Bonder-Ferrell and COMAN MLE methods for estimating attrition rates, the reader must gain a basic understanding of the overlying framework to which the attrition rates are applied. Lanchester-type models originated with the early works of F.W. Lanchester, a British engineer and inventor, in an attempt to quantify the advantages of concentrating fires in modern warfare. He hypothesized that ancient warfare was merely a collection of one-on-one duels where force size primarily determined battle outcomes. The resulting mathematical model representing this ancient form of warfare is referred to as Lanchester's Linear Law or Firer-Target | Firer-Target (FT|FT) attrition. On the other hand, Lanchester supposed that modern warfare maintained the ability to concentrate the effects of

multiple weapons on surviving targets, thus creating a many-on-one condition. In a hypothetical battle between forces $X$ and $Y$, this condition would make the force $X$ casualty rate proportional to the number of surviving firing systems in force $Y$. And, the resulting casualty-exchange ratio would be inversely proportional to the force ratio. This mathematical model for modern warfare conditions is termed Lanchester's Square Law or Firer | Firer (F|F) attrition. These underlying Lanchester models, with various extensions and improvements, supply the basic framework to the ATCAL Phase I and II algorithms, which will be discussed in Chapter IV.

## 1. Lanchester's Linear Law (FT|FT Attrition)

The primary assumption of ancient warfare is that any weapon system (soldier) not engaged in combat must wait until an enemy soldier becomes available before joining the battle. The assumption implies that the number of soldiers of force $X$ put forth on the battlefield to engage force $Y$ is determined by the number of soldiers of force $Y$ present. Therefore, under the conditions of ancient warfare, there should be no advantage to concentrating forces. A particular soldier from a force is either engaged in a one-on-one duel, or not. Intuitively, each force size is a function of time, where the continuous real time variables $x(t)$, $y(t)$, and $t$ are approximations to their discrete analogs in an actual battle. The change of each force size with respect to time depends upon the number of firers engaged in combat and can be represented mathematically by the (homogeneous) Lanchester Linear Law (FT|FT), Equations III.4 and III.5, where $\frac{dx}{dt}$ and $\frac{dy}{dt}$ represent the change in the size of forces $X$ and $Y$, respectively, over time.

$$\frac{dx}{dt} = -ax(t)y(t) \qquad \text{with } x(0) = x_0 \tag{III.4}$$

$$\frac{dy}{dt} = -bx(t)y(t) \qquad \text{with } y(0) = y_0 \tag{III.5}$$

$$x(t) = \text{size of force } X \text{ at time } t$$

$y(t)$ = size of force $Y$ at time $t$

$a$ = attrition rate at which an individual $Y$ firer kills $X$ targets

$b$ = attrition rate at which an individual $X$ firer kills $Y$ targets

## 2. Lanchester's Square Law (F|F Attrition)

Extending the assumptions of ancient warfare to modern battles, one gains the attribute that many firers can engage a single target, thus achieving the advantages associated with concentration of fires. Two general cases of combat developed out of this study, namely, area fire and aimed fire. First, Lanchester assumed area fire to be a situation where a force spreads its fires over a general area occupied by the enemy rather that aiming directly at individual enemy weapon systems. Assuming that these area fires are uniformly distributed over the target area and that the area is independent of the number of targets, the Lanchester Linear Law (FT|FT) was assumed to hold true for area fires. Second, aimed fire assumes that individual targets are identified and attacked by one or more opposing firers. In this case, Lanchester assumed that the attrition of force $X$ depended on how many force $Y$ firers were directing aimed fires at force $X$. Mathematically, the basic homogeneous form of Lanchester's Square Law (F|F) can be described by a system of differential equations, Equations III.6 and III.7, where $\frac{dx}{dt}$ and $\frac{dy}{dt}$ represent the change in the size of forces $X$ and $Y$, respectively, over time.

$$\frac{dx}{dt} = -ay(t) \qquad \text{with } x(0) = x_0 \qquad \text{(III.6)}$$

$$\frac{dy}{dt} = -bx(t) \qquad \text{with } y(0) = y_0 \qquad \text{(III.7)}$$

$x(t)$ = size of force $X$ at time $t$

$y(t)$ = size of force $Y$ at time $t$

$a$ = attrition rate at which an individual $Y$ firer kills $X$ targets

$b$ = attrition rate at which an individual $X$ firer kills $Y$ targets

The homogeneous representation of Lanchester's Square Law (F|F) can be extended to meet the needs of heterogeneous forces by accounting for all of the possible firer/target combinations in the simulated battle. The resulting heterogeneous formulation of Lanchester's Square Law (F|F) is provided by the system of differential equations, Equations III.8 and III.9, shown below.

$$\frac{dx_i}{dt} = -\sum_{j=1}^{n} a_{ij}\psi_{ij}y_j(t) \tag{III.8}$$

$$\frac{dy_j}{dt} = -\sum_{i=1}^{m} b_{ji}\Psi_{ji}x_i(t) \tag{III.9}$$

$x_i(t)$ = size of force $X$, system $i$, at time $t$

$y_j(t)$ = size of force $Y$, system $j$, at time $t$

$a_{ij}$ = attrition rate at which $Y_j$ firers kill $X_i$ targets

$\psi_{ij}$ = fraction of $Y_j$ firers allocated against $X_i$ targets

$b_{ji}$ = attrition rate at which $X_i$ firers kill $Y_j$ targets

$\Psi_{ji}$ = fraction of $X_i$ firers allocated against $Y_j$ targets

$X$ force = $\{x_1, x_2, x_3, \ldots, x_m\}$

$Y$ force = $\{y_1, y_2, y_3, \ldots, y_n\}$

The reader should be aware that Equations III.8 and III.9 represent one possible form of the Lanchester Square Law (F|F) equations. While the equations presented represent work which was primarily accomplished during the 1960s, the overall methodology has evolved over time. In the 1970s, fire allocation factors which influ-

ence the attrition rates were developed by submodels executed in support of the overall process. Nevertheless, the equations described above appear in a fundamental form which aids in the understanding of this topic.

### 3. The Significance of $a_{ij}$ and $b_{ji}$

As Lanchester's original purpose was a qualitative justification of the principle of concentration as an advantageous tactic in modern warfare, the derivation of the heterogeneous attrition rate coefficients $a_{ij}$ and $b_{ji}$ was of no particular concern. However, today, as Lanchester based attrition models are employed as part of theater level aggregated models, the significance of these attrition rates cannot be overemphasized. As part of the model verification process, current aggregated models must provide reasonable and quantitative results. These numerical values assigned to $a_{ij}$ and $b_{ji}$ are what represent the synergies of battle between various weapons systems and the very nature of specific actions on the battlefield. Their derivation is what brings believability to the equations present within combat models. Several methods have been proposed and utilized over the years to derive the attrition coefficients. The remaining background discussion of this chapter focuses on two of these methods of attrition rate estimation which are currently in use.

## D. THE BONDER-FERRELL METHOD FOR ATTRITION RATE ESTIMATION

The Bonder-Ferrell method for estimating attrition rates makes use of an independent analytical model which does not depend on input from other sources. Instead, a stochastic process model is developed for each $Y_j$ firing at a single passive type $X_i$ target, and the expected time between casualties ($E[T_{ij}^y]$) is determined, where $T_{ij}^y$ is a random variable representing the time it takes a single $Y_j$ firing system to kill one $X_i$ target. Assuming that the casualty process is a Markov (Poisson) process (see [Ref. 7]), the attrition rate parameters can then be expressed as $a_{ij} = \frac{1}{E[T_{ij}^y]}$ and

$b_{ji} = \frac{1}{E[T_{ji}^{x}]}$. While Bonder's original work focused on deriving the equation to compute $E[T]$ by calculating the distribution of the number of shots required to achieve a specified number of hits, Ferrell's extension of this work modeled this process as a Markov renewal process (see [Ref. 7]) with three discrete states (new engagement, hit, and miss) and the associated transition probabilities and times. Thus, the expected time required to kill an enemy target is the long run expected time required within the Markov renewal process until moving on to a new engagement. As early studies in this area focussed on homogeneous forces, continued work in the 1970s extended the concept to heterogeneous battles by combining conditional kill rates with target priority lists. Additionally, target acquisition was characterised as either parallel or serial.

One of the most significant advantages to the Bonder-Ferrell method of attrition coefficient estimation is that the computations are based upon what is going on in the battle at the given moment. There is no requirement to reference a data base library of high resolution simulation output to match up the conditions of battle between the overlying model and the high resolution battle. Additionally, since the underlying data used in these computations are basically measurable, the results are more credible to the user. This method is generally considered to be restrictive in that the in-depth engagement model is analytic, thus suppressing some detail. This form of attrition rate estimation also precludes the ability to capture synergistic effects of weapon system combinations as the underlying process does not account for weapon system interactions. The reliance upon engineering level data does lend this approach to the explicit definitions of engagements; however, the amount of data required on each weapon system is great. Relying upon closed form equations for the development of the $a_{ij}$ and $b_{ji}$, the Bonder-Ferrell method allows for the re-evaluation of the attrition coefficients at each time step of the simulation by simply recalling and recomputing the required input values.

## E. THE COMAN MAXIMUM LIKELIHOOD ESTIMATION (MLE) APPROACH TO ATTRITION RATE ESTIMATION

The COMAN MLE attrition estimation methodology is a fitted parameter model which examines the time series of casualty times (from a high resolution simulation) and computes the maximum likelihood estimate for the mean time between casualties. While other statistical methods exist for determining point estimates of this type (including the method of moments, Bayesian estimation, and the method of least squares), the MLE approach is the only method which has had any significant application in combat simulations [Ref. 8]. Similar to the Bonder-Ferrell approach, the COMAN MLE method relies upon the assumption that the time between casualties is a Markov (Poisson) process with the memoryless property (time until the next casualty does not depend upon the previous time before the last casualty). The COMAN MLE method is most easily explained by detailing its mathematical construct. The underlying assumption of this method is that the high resolution simulation data represents a sample from the continuous analogue to the deterministic homogeneous equations of Lanchester's Square Law (F|F) (see Equations III.6 and III.7), i.e., the continuous-parameter Markov chain with transition probabilities given by Equations III.10 and III.11 [Ref. 9].

$$\text{Prob}[X \text{ casualty in a small time interval of length } \Delta t] = an(t)\Delta t \tag{III.10}$$

$$\text{Prob}[Y \text{ casualty in a small time interval of length } \Delta t] = bm(t)\Delta t \tag{III.11}$$

$n(t)$ = the number of $Y$ combatants at time $t$

$m(t)$ = the number of $X$ combatants at time $t$

Additionally, consider the following random variable definitions and their associated properties required for the development of the MLE attrition coefficient estimation process. The reader can assume that any realization of a described random variables will be notationally represented by its corresponding lower-case letter.

$$C_k^X = \begin{cases} 1 & \text{if the } k^{th} \text{ casualty is an } X \text{ combatant,} \\ 0 & \text{otherwise,} \end{cases}$$

$$C_k^Y = \begin{cases} 1 & \text{if the } k^{th} \text{ casualty is an } Y \text{ combatant,} \\ 0 & \text{otherwise,} \end{cases}$$

$$c_T^X = \sum_{k=1}^{K} c_k^X \text{ total number of } X \text{ casualties}$$

$$c_T^Y = \sum_{k=1}^{K} c_k^Y \text{ total number of } Y \text{ casualties}$$

$$c_T^X + c_T^Y = K \text{ total number of } X \text{ and } Y \text{ casualties}$$

$$n(t_k) = \begin{cases} n_k & \text{the realization of the number of } Y \text{ combatants} \\ & \text{just after the occurrence of the } k^{th} \text{ casualty} \end{cases}$$

$$m(t_k) = \begin{cases} m_k & \text{the realization of the number of } X \text{ combatants} \\ & \text{just after the occurrence of the } k^{th} \text{ casualty} \end{cases}$$

Interpreting the random variable definitions given above, note that during the time interval $[t_k, t_{k+1}]$ there are $m_k$ $X$ combatants and $n_k$ $Y$ combatants alive for values of $k = (0, 1, 2, \ldots, K-1)$. Armed with high resolution simulation output data of the form $\{(t_1, c_1^X, c_1^Y), (t_2, c_2^X, c_2^Y), \ldots, (t_K, c_K^X, c_K^Y)\}$, the statistical estimates for the continuous time Markov chain representation of the deterministic form of Lanchester's Square Law (F|F) can be computed using the method of maximum likelihood estimation (MLE). As a battle develops, the casualty processes for the $X$ and $Y$ forces are simply two superimposed Poisson processes with respect to time (a random variable). Developing and maximizing these likelihood functions from their applicable joint probability density function (PDF) (representing the times between

casualties) will result in the derivation of the attrition rate estimates, $\hat{a}$ and $\hat{b}$. The maximum likelihood estimation process can be summarized by the steps detailed in Table X.

| | |
|---|---|
| Step 1 | Find the probability density function for the time until an $X$ casualty.<br>Find the probability density function for the time until a $Y$ casualty. |
| Step 2 | Construct the respective likelihood functions.<br>(i.e., the density functions for the observed sequences of events) |
| Step 3 | Determine the values of $\hat{a}$ and $\hat{b}$ that maximize the<br>respective likelihood functions. |

Table X. Maximum Likelihood Estimation Process Steps [Ref. 9]

## 1. Maximum Likelihood Estimation Steps

Applying the three maximum likelihood estimation steps to the stochastic representation of Lanchester's Square Law (F|F) represented by Equations III.10 and III.11 will result in the statistical derivation of $\hat{a}$ and $\hat{b}$. The author has chosen to detail the development of the estimated attrition parameters $\hat{a}$ and $\hat{b}$ from the $X$ casualty point of view. Initially, $C_k^X$ and $1 - C_k^X$ will be used to represent $X$ and $Y$ casualty occurrences, respectively.

*a. Step 1*

Let the random variable $S_X$ denote the time between $X$ casualties with the well-known exponential PDF $f_{S_X}(s_x) = an \exp^{-(an)s_x}$. Similarly, the PDF for the time between $Y$ casualties is $f_{S_Y}(s_y) = bm \exp^{-(bm)s_y}$. Further, let the random variable $S$ denote the time between any two consecutive casualties be defined as the minimum of $S_X$ and $S_Y$. The resulting PDF describing the time between any two casualties is

$$f_S(s) = (an + bm) \exp^{-(an+bm)s}. \qquad \text{(III.12)}$$

Incorporating the previously defined variable $C_k^X$, which equals one when the $k^{th}$ casualty is an $X$ combatant and zero when the $k^{th}$ casualty is a $Y$ combatant, one can further specify Equation III.12 above. Note that $C_k^X = 1$ if $S_X < S_Y$. The probability of this occurrence is $\text{Prob}(C_k^X = 1) = \dfrac{an}{an + bm}$. Likewise, a $Y$ casualty occurs if $S_X > S_Y$ which implies $C_k^X = 0$ and $\text{Prob}(C_k^X = 0) = \dfrac{bm}{an + bm}$. Therefore, the joint probability of the random variables $S$ and $C_k^X$ is

$$\begin{aligned} \text{Prob}(S \leq s, C_k^X = i) &= (1 - \exp^{-(an+bm)s}) \cdot \text{Prob}(c_k^X = i) \\ &\quad \text{where } 0 \leq s < \infty \text{ and } i = 0, 1 \\ &= (\frac{an}{an + bm})^{c_k^X} \cdot (\frac{bm}{an + bm})^{1-c_k^X} \cdot (1 - \exp^{-(an+bm)s}). \end{aligned}$$

Therefore, the representative joint PDF of $S$ and $C_k^X$ is

$$\begin{aligned} f_{S,C_k^X}(s, c_k^X) &= (\frac{an}{an + bm})^{c_k^X} \cdot (\frac{bm}{an + bm})^{1-c_k^X} \cdot (an + bm) \exp^{-(an+bm)s} \\ &= (an)^{c_k^X} (bm)^{1-c_k^X} \exp^{-(an+bm)s} \qquad \text{(III.13)} \\ &\quad \text{where } c_k^X = 0, 1. \end{aligned}$$

*b. Step 2*

The likelihood function is developed by considering that the $K$ casualties have occurred at times $(t_1, t_2, t_3, \ldots, t_K)$ with a total number of $X$ and $Y$ casualties represented by $c_T^X$ and $c_T^Y$, respectively, where $c_T^X + c_T^Y = K$. Recalling that $C_k^X = 1 \iff C_k^Y = 0$ and $C_k^X = 0 \iff C_k^Y = 1$, Equation III.13 can be functionally written as

$$(an_{k-1})^{c_k^X} (bm_{k-1})^{c_k^Y} \exp^{-(an_{k-1}+bm_{k-1})(t_k - t_{k-1})}. \qquad \text{(III.14)}$$

Equation III.14 represents the contribution of the $k^{th}$ casualty to the likelihood function. As the times between casualties are independent random variables, the likelihood function for the observed sequence of events, Equation III.15, is the product of all of the independent contributions.

$$L(a,b) = \prod_{k=1}^{K} (an_{k-1})^{c_k^X} (bm_{k-1})^{c_k^Y} \exp^{-(an_{k-1}+bm_{k-1})(t_k-t_{k-1})} \tag{III.15}$$

*c. Step 3*

Finally, the COMAN MLE process requires the maximization of this likelihood function. However, it is a common mathematical practice to maximize the natural logarithm (ln) of the likelihood function as detailed below by Equation III.16. Both maximum values will occur at the same point [Ref. 10] and the logarithmic form is more easily manipulated.

$$\ln[L(a,b)] = \sum_{k=1}^{K} c_k^X \ln(an_{k-1}) + \sum_{k=1}^{K} c_k^Y \ln(bm_{k-1}) - \sum_{k=1}^{K} (an_{k-1} + bm_{k-1})(t_k - t_{k-1}) \tag{III.16}$$

Continuing with Step 3, one can take the partial derivatives of Equation III.16 with respect to $a$ and $b$ to get Equations III.17 and III.18, respectively.

$$\frac{\partial \ln[L(a,b)]}{\partial a} = \frac{c_T^X}{a} - \sum_{k=1}^{K} n_{k-1}(t_k - t_{k-1}) \tag{III.17}$$

$$\frac{\partial \ln[L(a,b)]}{\partial b} = \frac{c_T^Y}{b} - \sum_{k=1}^{K} m_{k-1}(t_k - t_{k-1}) \tag{III.18}$$

Finally, maximize Equations III.17 and III.18 by setting each of the partial derivatives equal to zero and solving for $a$ and $b$. The resulting solutions for $a$ and $b$, denoted $\hat{a}$ and $\hat{b}$, maximize the likelihood function (Equation III.15) and serve as the COMAN MLE estimates for the attrition rate coefficients. See Equations III.19 and III.20.

$$\hat{a} = \frac{c_T^X}{\sum_{k=1}^{K} n_{k-1}(t_k - t_{k-1})} \tag{III.19}$$

$$\hat{b} = \frac{c_T^Y}{\sum_{k=1}^{K} m_{k-1}(t_k - t_{k-1})} \tag{III.20}$$

## 2. Summary of the COMAN MLE Method

While the presented mathematical description of the COMAN MLE method for estimating attrition rate coefficients is applicable only to the homogeneous representation of Lanchester's Square Law (F|F) in one of its simpler forms, the reader can see that the general method is quite simplistic. One of the simplifying characteristics of the developed example is the appearance of the attrition rate coefficients as linear terms only. It is quite possible that the true nature of the attrition rate coefficients is non-linear in actual combat; however, for the purposes of this discussion, the author has chosen to represent the mathematics of the method with tractable forms. As a practical example, Appendix C details the application of the COMAN MLE method for attrition rate estimation to the high resolution output data from the AOAC 97-3 Janus Simulation described in Chapter II. The calculations are presented for the mechanized battle between the BLUEFOR M2 (with TOW missile) and REDFOR BMP-2 (with AT-5 missile). Note that this computational excursion makes use of Lanchester's Square Law (F|F) (as the mechanized battle is one char-

acterized by exchanges of aimed fire) and the mathematical framework leading up to and including Equations III.19 and III.20.

## F. EXTENSION OF ATTRITION RATE CONCEPTS TO THE ATCAL ALGORITHMS

By no means should the reader consider this treatment of attrition rate analysis to be exhaustive. A significant number of noteworthy modifications have been proposed and are used within Lanchester-type deterministic models. For a highly detailed inspection of these modifications, the interested reader should consult the prolific works of Professor James G. Taylor, Naval Postgraduate School, and co-advisor to this research. However, with the general background development of the methods for attrition rate estimation complete, the reader is now prepared to consider their application to (or lack thereof) the ATCAL algorithms. The specific modifications to the underlying Lanchester-type model which form the basis for the ATCAL methodology can be primarily attributed to Gordon M. Clark and his PhD Thesis, "The Combat Analysis Model" [Ref. 8], while ongoing analysis is being conducted by James G. Taylor [Ref. 2]. However, recall that the specific attrition rate parameter estimation process used in ATCAL Phase I can be described as an *ad hoc* process at best.

# IV. THE UNDERLYING LANCHESTER-TYPE MODEL FOR ATCAL

As the primary purpose of this research is to establish a test mechanism for evaluating the current ATCAL attrition algorithm as it applies to aggregated combat models (like CEM and TACWAR), the interested reader must develop a familiarity with ATCAL's underlying Lanchester-type models and their application via explicit assessment equations. As detailed documentation describing the theoretical bases of ATCAL is not available from its original author, this chapter attempts to outline the construct of the ATCAL attrition algorithm based primarily upon a very thorough treatment of the subject by James G. Taylor. [Ref. 2] It is with an understanding of the current ATCAL algorithm that the interested reader could conduct research for improving its mathematical efficiency or developing mathematical variants to fulfill other combat model requirements. The reader may find it helpful to review Chapter III, Section C, which details the basic framework of Lanchester's Linear (FT|FT) and Square (F|F) Laws because of the parallelisms which extend to the Lanchester-type models present in the ATCAL attrition algorithm.

## A. THE HOMOGENEOUS FORCE MODEL

Considering the case of homogeneous combat between two opposing forces, the ATCAL attrition algorithm employs the nonlinear Equations IV.1 and IV.2 which can be attributed to Gordon M. Clark [Ref. 8].

$$\frac{dx}{dt} = -\alpha(1 - p^{x(t)})y(t) \qquad \text{with } x(0) = x_0 \tag{IV.1}$$

$$\frac{dy}{dt} = -\beta(1 - q^{y(t)})x(t) \qquad \text{with } y(0) = y_0 \tag{IV.2}$$

$x(t) > 0$ size of force $X$ at time $t$

| | |
|---|---|
| $y(t) > 0$ | size of force $Y$ at time $t$ |
| $\alpha > 0$ | rate at which an individual $Y$ firer kills acquired $X$ targets |
| $\beta > 0$ | rate at which an individual $X$ firer kills acquired $Y$ targets |
| $0 \leq p^{x(t)} \leq 1$ | probability that an individual $Y$ firer has no $X$ target available for engagement |
| $0 \leq q^{y(t)} \leq 1$ | probability that an individual $X$ firer has no $Y$ target available for engagement |

The reader may find it more convenient to express Equations IV.1 and IV.2 with respect to target availabilities rather than non availabilities. To do so, let $1-(1-A)^{x(t)} = 1 - p^{x(t)}$, which is the probability that an individual $Y$ firer has one or more $X$ target(s) available for engagement. And, analogously, let $1-(1-B)^{y(t)} = 1-q^{y(t)}$. With these substitutions, Equations IV.1 and IV.2 can be expressed as follows.

$$\frac{dx}{dt} = -\alpha[1-(1-A)^{x(t)}]y(t) \qquad \text{with } x(0) = x_0 \qquad \text{(IV.3)}$$

$$\frac{dy}{dt} = -\beta[1-(1-B)^{y(t)}]x(t) \qquad \text{with } y(0) = y_0 \qquad \text{(IV.4)}$$

Considering the elements of Equation IV.3, the reader will note that the multiplication of the conditional kill rate ($\alpha$) with the probability of target availability ($1-(1-A)^{x(t)}$) produces the expected rate at which an individual $Y$ firer kills $X$ targets. Similarly, the multiplication of $\beta$ and $1-(1-B)^{y(t)}$ yields the expected rate at which an individual $X$ firer kills $Y$ targets.

It has been shown that force levels can never become zero or negative as a matter of theory (see [Ref. 9]). However, as the attrition calculations are necessarily executed on computer platforms, the potential for achieving "computer zero" must be recognized. So, in practice, the attrition models above must be defined to be valid only when the forces levels, $x(t)$ and $y(t)$ are greater than zero. This refinement of the

homogeneous attrition model within the ATCAL algorithm produces Equations IV.5 and IV.6.

$$\frac{dx}{dt} = \begin{cases} -\alpha[1-(1-A)^{x(t)}]y(t) & \text{for } x(t), y(t) > 0, \\ 0 & \text{otherwise.} \end{cases} \tag{IV.5}$$

$$\frac{dy}{dt} = \begin{cases} -\beta[1-(1-B)^{y(t)}]x(t) & \text{for } x(t), y(t) > 0, \\ 0 & \text{otherwise.} \end{cases} \tag{IV.6}$$

This positive force level requirement can be easily incorporated in computer algorithms by including a conditional check of the current force level minus any calculated change to the force level. If the resulting force level is less than zero, then the algorithm should return a value of zero. Otherwise, the current force level is updated by subtracting the calculated attrition.

## 1. Application of the Averaging Operator

In order to transform Equations IV.5 and IV.6 into explicit assessment equations as employed in the ATCAL algorithm, it is important to develop the mathematical properties of the averaging operator (over time) given by

$$Ave[x] = \bar{x} = \frac{1}{t}\int_0^t x(s)ds \tag{IV.7}$$

where $x(t)$ is a function of time.

Application of this operator to the Lanchester-type equations developed above will result in an operator equation for the force levels, $x(t)$ and $y(t)$, respectively. Define the number of casualties inflicted on the $X$ force as $\Delta x$ and the number of casualties inflicted on the $Y$ force as $\Delta y$.

$$\Delta x = x_0 - x(t), \qquad \text{where } x_0 = x(0)$$

$$\Delta y = y_0 - y(t), \qquad \text{where } y_0 = y(0)$$

Now, consider applying the averaging operator to $\frac{dx}{dt}$ which results in

$$Ave[\frac{dx}{dt}] = \frac{1}{t}\int_0^t \frac{dx}{ds}\cdot ds$$

$$
\begin{aligned}
&= \frac{1}{t}[x(t) - x_0] \\
&= -\frac{[x_0 - x(t)]}{t} \\
&= -\frac{\Delta x}{t}.
\end{aligned}
$$

Hence, applying the averaging operator to the homogeneous Lanchester-type Equations IV.5 and IV.6 representative of the ATCAL algorithm, one obtains the operator equations, Equations IV.8 and IV.9 below.

$$
\begin{aligned}
\frac{dx}{dt} &= -\alpha[1 - (1 - A)^{x(t)}]y(t) \\
\Longleftrightarrow Ave[\frac{dx}{dt}] &= Ave[-\alpha[1 - (1 - A)^{x(t)}]y(t)] \\
\Longleftrightarrow -\frac{\Delta x}{t} &= -\alpha Ave[[1 - (1 - A)^{x(t)}]y(t)] \\
\Longleftrightarrow \Delta x &= \alpha t Ave[[1 - (1 - A)^{x(t)}]y(t)] \qquad \text{(IV.8)}
\end{aligned}
$$

and, similarly,

$$
\Delta y = \beta t Ave[[1 - (1 - B)^{y(t)}]x(t)]. \qquad \text{(IV.9)}
$$

The reader will note that the arguments of the averaging function appearing in Equations IV.8 and IV.9 above are highly nonlinear. Unfortunately, these equations cannot be further simplified to explicit expressions involving only average force levels without making some type of approximation. The key approximation made within the ATCAL algorithm is that the average of this nonlinear argument in $x(t)$ and $y(t)$ is equal to the same functional relationship between $\bar{x}$ and $\bar{y}$, the results of the averaging function applied to $x(t)$ and $y(t)$. Although this approximation is not precise, it is often applied to simplify averages of nonlinear functional relationships. It is this simplification that allows ATCAL to move forward computationally. Equations IV.8 and IV.9 can now be replaced by Equations IV.10 and IV.11.

$$
\Delta x = \alpha t[1 - (1 - A)^{\bar{x}}]\bar{y} \qquad \text{(IV.10)}
$$

$$\Delta y = \beta t[1-(1-B)^{\bar{y}}]\bar{x} \qquad \text{(IV.11)}$$

$\bar{x}$ = time average of the force level $x(t)$

$\bar{y}$ = time average of the force level $y(t)$

$\Delta x$ = number of $X$ casualties during time $t$

$\Delta y$ = number of $Y$ casualties during time $t$

## 2. Applying the Results for Homogeneous Forces

As written, Equations IV.10 and IV.11 have four unknown quantities, namely, the average force levels ($\bar{x}$ and $\bar{y}$) and the numbers of casualties ($\Delta x$ and $\Delta y$). With two equations and four unknowns, additional assumptions are required in order to solve this system of assessment equations. The second key assumption made in the ATCAL algorithm is that average force levels can be represented by the expressions $\bar{x} = \frac{(-\Delta x)}{ln(1-\frac{\Delta x}{x_0})}$ and $\bar{y} = \frac{(-\Delta y)}{ln(1-\frac{\Delta y}{y_0})}$. [Ref. 11] It so happens that these expressions hold true, respectively, if $x(t)$ and $y(t)$ are exponential functions (increasing or decreasing) over time. As force levels necessarily decrease during battle, the negative exponential function is assumed. Combining this information with Equations IV.10 and IV.11, the underlying Lanchester-type attrition model used to determine the numbers of casualties during each assessment period is represented in the ATCAL algorithm by the following system of four simultaneous nonlinear equations in the four unknowns, $\bar{x}, \bar{y}, \Delta x$, and $\Delta y$.

$$\begin{cases} \Delta x = \alpha t[1-(1-A)^{\bar{x}}]\bar{y} \\ \Delta y = \beta t[1-(1-B)^{\bar{y}}]\bar{x} \\ \bar{x} = \frac{(-\Delta x)}{ln(1-\frac{\Delta x}{x_0})} \\ \bar{y} = \frac{(-\Delta y)}{ln(1-\frac{\Delta y}{y_0})} \end{cases}$$

While small perturbations of this notation are explicitly modeled in the ATCAL algorithm, this system of equations should be thought of as the basic ATCAL casualty

assessment system of equations. This form better suits future research in applying numerical solution techniques to solve the system (recognizing the requirement for excluding negative force levels as described in Equations IV.5 and IV.6). The actual method used in ATCAL to solve this system of nonlinear equations is a heuristic form of successive substitutions which is beyond the scope of this research. The interested reader may find the study of alternative numerical solution techniques extremely relevant to verifying current ATCAL methodologies and proposing future replacement ones.

## B. THE HETEROGENEOUS FORCE MODEL

Considering the case of heterogeneous combat between two opposing forces made up of $m$ distinct $X$ force weapon systems and $n$ distinct $Y$ force weapon systems, the ATCAL attrition algorithm employs the nonlinear Clark Equations IV.12 and IV.13 detailed below. In these equations, $i = 1$ denotes the lowest priority target type and $i = m$ denotes the highest priority target type within the $X$ force. And, $j = 1$ denotes the lowest priority target type and $j = n$ denotes the highest priority target type within the $Y$ force. Again, the reader may find it helpful to compare these equations with Equations III.8 and III.9 of Chapter III.

$$\frac{dx_i}{dt} = -\sum_{j=1}^{n} \alpha_{ij}(1 - p_{ij}^{x_i(t)}) \prod_{k=i+1}^{m} p_{kj}^{x_k(t)} y_j(t) \qquad \text{for } i = 1, 2, \cdots, m \tag{IV.12}$$

$$\frac{dy_j}{dt} = -\sum_{i=1}^{m} \beta_{ji}(1 - q_{ji}^{y_j(t)}) \prod_{k=j+1}^{n} q_{ki}^{y_k(t)} x_i(t) \qquad \text{for } j = 1, 2, \cdots, n \tag{IV.13}$$

$x_i(t) > 0$ number of weapon systems of type $i$ in force $X$ at time $t$

$y_j(t) > 0$ number of weapon systems of type $j$ in force $Y$ at time $t$

$x_i(0) = x_{i0}$ for $i = 1, 2, \cdots, m$

$y_j(0) = y_{j0}$ for $j = 1, 2, \cdots, n$

$\alpha_{ij} > 0$ rate at which an individual $Y_j$ firer kills acquired $X_i$ targets

$\beta_{ji} > 0$ rate at which an individual $X_i$ firer kills acquired $Y_j$ targets

$0 \leq p_{ij}^{x_i(t)} \leq 1$ probability that an individual $Y_j$ firer has no $X_i$ target available for engagement

$0 \leq q_{ji}^{y_j(t)} \leq 1$ probability that an individual $X_i$ firer has no $Y_j$ target available for engagement

Similar to the homogeneous case, the reader may find it more convenient to express Equations IV.12 and IV.13 in terms of target availabilities by letting $1-(1-A_{ij})^{x_i(t)} = 1 - p_{ij}^{x_i(t)}$ and $1 - (1 - B_{ji})^{y_j(t)} = 1 - q_{ji}^{y_j(t)}$. With this substitution, Equations IV.12 and IV.13 can be expressed as follows.

$$\frac{dx_i}{dt} = -\sum_{j=1}^{n} \alpha_{ij}\{(1-(1-A_{ij})^{x_i(t)}) \prod_{k=i+1}^{m} (1-A_{kj})^{x_k(t)}\} y_j(t) \qquad i = 1, 2, \cdots, m \tag{IV.14}$$

$$\frac{dy_j}{dt} = -\sum_{i=1}^{m} \beta_{ji}\{(1-(1-B_{ji})^{y_j(t)}) \prod_{k=j+1}^{n} (1-B_{ki})^{y_k(t)}\} x_i(t) \qquad j = 1, 2, \cdots, n \tag{IV.15}$$

Again, in order to preclude the possibility of achieving "machine zero" (or negative force levels) during numerical attrition calculations, Equations IV.14 and IV.15 can be further specified so that the force levels $x_i(t)$ and $y_j(t)$ are valid only when they are greater than zero. One final notational simplification renders the heterogeneous formulation of the underlying Lanchester-type model for ATCAL more compact. Consider the set of indices corresponding to target types with a higher priority than a given target type by formally defining

$I_{ij} = \{k | k \in integers\}$

$X$ target type $k$ has a higher priority than target type $i$ for a $Y_j$ firer; and,

$J_{ji} = \{k | k \in integers\}$

$Y$ target type $k$ has a higher priority than target type $j$ for a $X_i$ firer.

With this simplifying set notation, a preferred form for the underlying Lanchester-type equations for ATCAL appear below in Equations IV.16 and IV.17. This relatively simple representation results in less computational requirements when implemented as the attrition model of a large-scale aggregated combat model.

$$\frac{d_i x}{dt} = \begin{cases} -\sum_{j=1}^{n} \alpha_{ij} \{(1 - p_{ij}^{x_i(t)}) \prod_{k \in I_{ij}} p_{kj}^{x_k(t)}\} y_j(t) & \text{for } x_i(t), y_j(t) > 0, \\ 0 & \text{otherwise.} \end{cases} \tag{IV.16}$$

$$\frac{d_j y}{dt} = \begin{cases} -\sum_{i=1}^{m} \beta_{ji} \{(1 - q_{ji}^{y_j(t)}) \prod_{k \in J_{ji}} q_{ki}^{y_k(t)}\} x_i(t) & \text{for } x_i(t), y_j(t) > 0, \\ 0 & \text{otherwise.} \end{cases} \tag{IV.17}$$

## 1. Application of the Averaging Operator

Without loss of generality, the application of the averaging operator (with associated notational definitions) to the heterogeneous Lanchester-type equations will result in operator equations for the force levels, $x_i(t)$ and $y_j(t)$. In order to maintain consistent notation, the author has chosen to represent the equations using the "target availability" notation of Equations IV.14 and IV.15.

$$\begin{aligned} \frac{dx_i}{dt} &= -\sum_{j=1}^{n} \alpha_{ij} \{(1 - (1 - A_{ij})^{x_i(t)}) \prod_{k=i+1}^{m} (1 - A_{kj})^{x_k(t)}\} y_j(t) \\ \iff Ave[\frac{dx_i}{dt}] &= Ave[-\sum_{j=1}^{n} \alpha_{ij} \{(1 - (1 - A_{ij})^{x_i(t)}) \prod_{k=i+1}^{m} (1 - A_{kj})^{x_k(t)}\} y_j(t)] \\ \iff -\frac{\Delta x_i}{t} &= -\sum_{j=1}^{n} \alpha_{ij} Ave[\{(1 - (1 - A_{ij})^{x_i(t)}) \prod_{k=i+1}^{m} (1 - A_{kj})^{x_k(t)}\} y_j(t)] \\ \iff \Delta x_i &= t \sum_{j=1}^{n} \alpha_{ij} Ave[\{(1 - (1 - A_{ij})^{x_i(t)}) \prod_{k=i+1}^{m} (1 - A_{kj})^{x_k(t)}\} y_j(t)] \end{aligned} \tag{IV.18}$$

and, similarly,

$$\Delta y_j = t\sum_{i=1}^{m}\beta_{ji}Ave[\{(1-(1-B_{ji})^{y_j(t)})\prod_{k=j+1}^{n}(1-B_{ki})^{y_k(t)}\}x_i(t)]. \tag{IV.19}$$

Analogous to the homogeneous case, the key approximation made within the ATCAL algorithm is that the average of these nonlinear arguments in $x_i(t)$ and $y_j(t)$ are equal to the same functional relationships between $\bar{x}_i$ and $\bar{y}_j$, which are the results of the averaging function applied to $x_i(t)$ and $y_j(t)$. Applying this approximation, Equations IV.18 and IV.19 can be replaced by Equations IV.20 and IV.21.

$$\Delta x_i = t\sum_{j=1}^{n}\alpha_{ij}\{(1-(1-A_{ij})^{\bar{x}_i})\prod_{k=i+1}^{m}(1-A_{kj})^{\bar{x}_k}\}\bar{y}_j \tag{IV.20}$$

$$\Delta y_j = t\sum_{i=1}^{m}\beta_{ji}\{(1-(1-B_{ji})^{\bar{y}_j})\prod_{k=j+1}^{n}(1-B_{ki})^{\bar{y}_k}\}\bar{x}_i \tag{IV.21}$$

## 2. Applying the Results for Heterogeneous Forces

Similar to the homogeneous argument presented in the previous section, both the average force levels ($\bar{x}_i$ and $\bar{y}_j$)and the numbers of casualties ($\Delta x_i$ and $\Delta y_j$) are unknowns in Equations IV.20 and IV.21. Therefore, this system is made up of $(m+n)$ nonlinear equations in $2\cdot(m+n)$ unknowns. In order to increase the number of equations to equal the number of unknowns , ATCAL again makes use of an assumption for the average force levels resulting in the expressions $\bar{x}_i = \frac{(-\Delta x_i)}{ln(1-\frac{\Delta x_i}{x_{i0}})}$ and $\bar{y}_j = \frac{(-\Delta y_j)}{ln(1-\frac{\Delta y_j}{y_{j0}})}$. [Ref. 11] Combining this information with Equations IV.20 and IV.21, the underlying Lanchester-type attrition model used to determine the numbers of casualties during each assessment period is represented in the ATCAL algorithm as the following system of $2\cdot(m+n)$ simultaneous nonlinear equations in the $2\cdot(m+n)$ unknowns, $\bar{x}_i, \bar{y}_j, \Delta x_i$, and $\Delta y_j$.

$$\begin{cases} \Delta x_i &= t\sum_{j=1}^{n}\alpha_{ij}\{(1-(1-A_{ij})^{\bar{x}_i})\prod_{k=i+1}^{m}(1-A_{kj})^{\bar{x}_k}\}\bar{y}_j \\ \Delta y_j &= t\sum_{i=1}^{m}\beta_{ji}\{(1-(1-B_{ji})^{\bar{y}_j})\prod_{k=j+1}^{n}(1-B_{ki})^{\bar{y}_k}\}\bar{x}_i \\ \bar{x}_i &= \frac{(-\Delta x_i)}{ln(1-\frac{\Delta x_i}{x_{i0}})} \\ \bar{y}_j &= \frac{(-\Delta y_j)}{ln(1-\frac{\Delta y_j}{y_{j0}})} \end{cases}$$

While small perturbations of this notation are explicitly modeled in the ATCAL algorithm, this system of equations should be thought of as the basic ATCAL caualty assessment equations. This form better suits future research in applying numerical solution techniques to solve the system (recognizing the requirement for excluding negative force levels as described in Equations IV.16 and IV.17). The actual method used in ATCAL to solve this system of nonlinear equations is a heuristic form of successive substitutions which is beyond the scope of this research. The interested reader may find the study of alternative numerical solution techniques extremely relevant to verifying current ATCAL methodologies and proposing future replacement ones.

## C. SUMMARY OF THE LANCHESTER-TYPE ASSESSMENT EQUATIONS IN ATCAL

The homogeneous and heterogeneous systems of nonlinear equations found at the ends of Sections A and B, respectively, comprehensively describe the underlying Lanchester-type models and their basic assessment equations for the ATCAL attrition methodology. "The most significant implication of these results, however, is that a much more convenient way of generating numerical results for ATCAL has immediately been established: namely, numerical integration of the underlying Lanchester-type differential equations." [Ref. 2] Moreover, with these mathematical constructs, the interested reader is now prepared to further investigate the soundness of the heuristic successive substitution method of ATCAL and compare it to more robust numerical solution techniques.

# V. CONCLUSION

## A. CONCLUSIONS

This research has developed a practical test mechanism for studying the attrition methodologies of aggregated combat models. The Janus high resolution simulation software, capable of modeling brigade sized (and below) operations, is completely adequate for producing the required high resolution output data required for the analysis of aggregated attrition methodologies. Janus is both widely available within the military community (to include the Naval Postgraduate School) and is easily learned through the use of a tutorial. See [Ref. 5]. This user friendly computer simulation provides the researcher with sufficient detail and a mechanism for capturing detailed interactions on the modeled battlefield. The ability to capture the highly detailed interactions between weapon systems is what qualifies Janus as a valuable tool for conducting analysis of the attrition algorithms inherent to ATCAL (and other aggregated attrition methodologies). The reader should follow the steps outlined in Section C to initiate such a study.

## B. RECOMMENDATIONS

First, having established the vehicle (Janus) for generating the data required for developing attrition (kill) rate parameters, the author has opened the door for continued research in the area of attrition methodologies. As this research developed and discussed one such combat scenario, the continued study of attrition calculations would require additional Janus scenarios with varying parameters. The creation and execution of such scenarios could easily be incorporated into current high resolution modeling courses taught at the Naval Postgraduate School.

Second, as discussed in Chapter IV, the nonlinear attrition assessment equations resulting from the Lanchester-type equations used in the ATCAL algorithm are currently "solved" using a heuristic method of successive substitutions. Significant

follow-on research is applicable in the employment of a more robust numerical solution technique for these systems of equations. This area of continued study does not necessarily depend upon additional Janus scenarios; however, additional scenarios would provide a data source for technique verification.

Third, the computer code which contains the ATCAL Phase I and II algorithms exists in several mediums. A significant endeavor integral to making ATCAL (and any proposed modifications) more efficient includes a thorough analysis of the current computer code which exists in at least two languages, FORTRAN and C. The interested reader may find that the algorithms, which make up ATCAL would be more efficient in one or more specific computer languages. For example, a proposed numerical solution technique may be more conducive to one computer language than another.

Finally, an automated bridge is required between the Janus high resolution output data and the computer code used to perform the aggregated attrition calculations (like ATCAL). While this capability may not be directly applicable to the actual execution of aggregated models as they currently exist, it is integral to the efficient study of the algorithms themselves. It is in the research arena that this automated capability for linking Janus output to attrition algorithms would be helpful. JETS may be an important tool for continued study of this recommendation.

As combat models are an integral part of the military analysis and training communities, continued analysis of attrition methodologies (specifically ATCAL) in the field of aggregated combat modeling will greatly enhance model believability and overall usefulness. As computer technologies continue to outpace attrition algorithm development, verification, and validation, a continued focus towards efficiency and accuracy will ensure the applicability of current and future attrition methodologies.

## C. INITIATION OF ATTRITION ANALYSIS USING JANUS

The key to initiating a detailed study of attrition and its inherent algorithms lies within the generation of high resolution combat simulation data. As such, the researcher must carefully consider the process of creating high resolution scenarios. The interested researcher should consider the following steps which outline the model formulation and data collection process.

| | |
|---|---|
| Step 1 | Define the tactical scenario (forces composition, terrain type, environmental conditions, and concept of the operation) for which a model is desired. |
| Step 2 | Construct the Janus simulation scenario and validate its representation of the desired interaction between modeled forces. |
| Step 3 | Determine an appropriate number ($n$) of iterations for which to execute the Janus simulation. |
| Step 4 | Independently execute the Janus simulation $n$ times to develop a robust sample of simulation output data from which statistically significant killer/victim information can be determined. |
| Step 5 | Analyze the consolidated high resolution output data and estimate the attrition (kill) rates between opposing weapons systems. |
| Step 6 | Incorporate the derived attrition (kill) rates in the analysis of attrition algorithms inherent to ATCAL (and other aggregated attrition methodologies). |
| Step 7 | Utilize an appropriate Lanchester-type deterministic model to replay the simulated battle. |

Table XI. Steps for Attrition Analysis and Deterministic Battle Replay Using Janus

# LIST OF REFERENCES


[1] James K. Hartman, Sam H. Parry, and William J. Caldwell. *Aggregated Combat Modeling.* Naval Postgraduate School, Monterey, California, 1992.

[2] James G. Taylor. *Working Papers, SAC of OSD PA & E Project.* 1997-1998.

[3] Titan. Applications Group Inc. *The Janus 3.X/UNIX Model User's Manual.* Fort Leavenworth, Kansas, 1993.

[4] Robert Gordon. *Janus Brigade Simulation, AOAC 97-3 (software).* Fort Knox, Kentucky, 1997.

[5] Bard K. Mansager, Gerald M. Pearman, Larry R. Larimer, and Michael L. Shenk. *Janus Version 6.0 Tutorial.* Number NPS-MA-97-007. December 5 1997.

[6] Small Group 2 Armor Officer Advanced Course. *52d Infantry Division (Mechanized) Operations Order 97-06-01.* June 1 1997.

[7] Sheldon M. Ross. *Introduction to Probability Models.* Academic Press, Inc., San Diego, California, 1993.

[8] Gordon M. Clark. *The Combat Analysis Model.* Columbus, Ohio, 1969.

[9] James G. Taylor. *Lanchester Models of Warfare, Volume II.* March 1983.

[10] Richard J. Larsen and Morris L. Marx. *An Introduction to Mathematical Statistics and Its Applications.* Prentice-Hall, Englewood Cliffs, New Jersey, 1986.

[11] U.S. Army Concepts Analysis Agency (CAA). *ATCAL: An Attrition Model Using Calibrated Parameters.* Technical Paper 83-3, Bethesda, Maryland, 1983.

[12] Gilbert Strang. *Linear Algebra and Its Applications.* Harcourt Brace & Company, Orlando, Florida, 1988.

[13] William E. Boyce and Richard C. DiPrima. *Elementary Differential Equations and Boundary Value Problems.* John Wiley & Sons, Inc., New York, New York, 1992.

# APPENDIX A. JANUS COMBATANTS LISTING AND RUN-TIME BATTLEFIELD PICTURES

This Appendix provides the reader with the detailed description of the combat systems making up the REDFOR and BLUEFOR modeled in the AOAC 97-3 Janus Simulation described in Chapter II. Additionally, pictures are included to depict the battlefield details and force allocations prior to the start of hostilities and at 30 minute increments throughout the simulation.

| | |
|---|---|
| T-80 Main Battle Tank | 15 |
| BMP-2 Armored Personnel Carrier | 55 |
| BRDM-A Armored Personnel Carrier | 10 |
| BRDM-2 Armored Personnel Carrier | 7 |
| GMZ-MI Armored Mine Warfare System | 2 |
| MTK_LI Armored Engineer System | 1 |
| 2S12 M 122mm Self-Propelled Artillery | 16 |
| IF TRU Wheeled Truck | 26 |
| DF Tru Wheeled Truck | 16 |
| 2S1 155mm Self-Propelled Artillery | 30 |
| BM-21 Rocket Launcher | 8 |
| SNAR-2 Radar | 2 |
| ZOOPAR Radar | 2 |
| 2S5 152mm Self-Propelled Artillery | 36 |
| ADA TM Air Defense Artillery Team | 5 |
| ZSU-23 Air Defense Artillery | 3 |
| HIND Attack Helicopter | 6 |
| POL AI Aviation Fuel Depot | 2 |
| **Total REDFOR Combatants** | 242 |

Table XII. REDFOR Organization for AOAC 97-3 Janus Simulation

| | |
|---|---|
| M1A1 Main Battle Tank | 82 |
| M1A1P Main Battle Tank w/ Mine Plow | 24 |
| M1A1R Main Battle Tank w/ Mine Roller | 8 |
| M2 Armed Armored Personnel Carrier | 113 |
| BSFV Armed Improved Armored Personnel Carrier | 6 |
| M113 Armored Personnel Carrier | 21 |
| FIST-V Artillery Command Vehicle | 4 |
| CEV Combat Engineer Vehicle | 4 |
| BRIDGE Mobile Bridge Carrier | 5 |
| ADA TE Air Defense Artillery Team | 4 |
| ACE Armored Combat Earthmover | 13 |
| AVLM Armored Vehicle Launched Bridge | 9 |
| AVLM-W Armored Vehicle Launched Bridge | 6 |
| AVLB W Armored Vehicle Launched Bridge | 2 |
| HMV.50 Wheeled Vehicle | 47 |
| HMV/M1 Wheeled Vehicle | 10 |
| HMV/SM Wheeled Vehicle | 6 |
| HMV/CO Wheeled Vehicle | 8 |
| IF TRU Wheeled Truck | 25 |
| DF Tru Wheeled Truck | 4 |
| M106A1 120mm Mortar Vehicles | 22 |
| M577 Armored Personnel Carrier (Command) | 6 |
| GSR/M1 Ground Surveillance Radar | 1 |
| SCT TE Scout Team | 34 |
| SAPPER Combat Engineer Team | 90 |
| SAW TE Machine Gun Team | 144 |
| VOLCANO Mine Dispensing System | 4 |
| M109A3 155mm Self-Propelled Artillery | 24 |
| M109A6 155mm Self-Propelled Artillery | 18 |
| HMMQ36 Artillery Radar System | 1 |
| ADA TE Air Defense Artillery Team | 4 |
| SMK113 Armored Vehicle Smoke Generator | 3 |
| A-10 Fixed Wing Close Air Support | 12 |
| **Total BLUEFOR Combatants** | 764 |

Table XIII. BLUEFOR Organization for AOAC 97-3 Janus Simulation

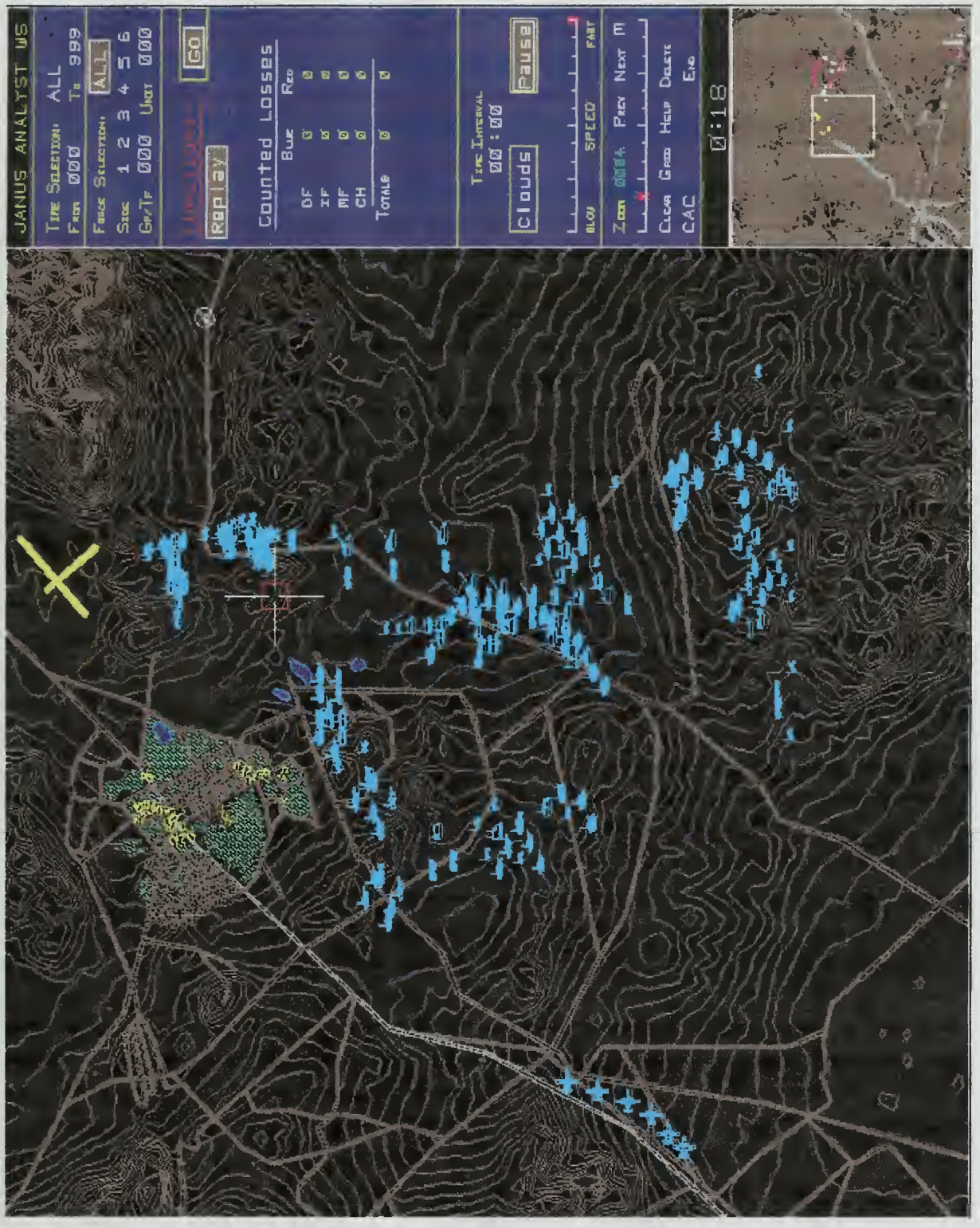


Figure 1. BLUEFOR Initial Disposition for AOAC 97-3 Janus Simulation

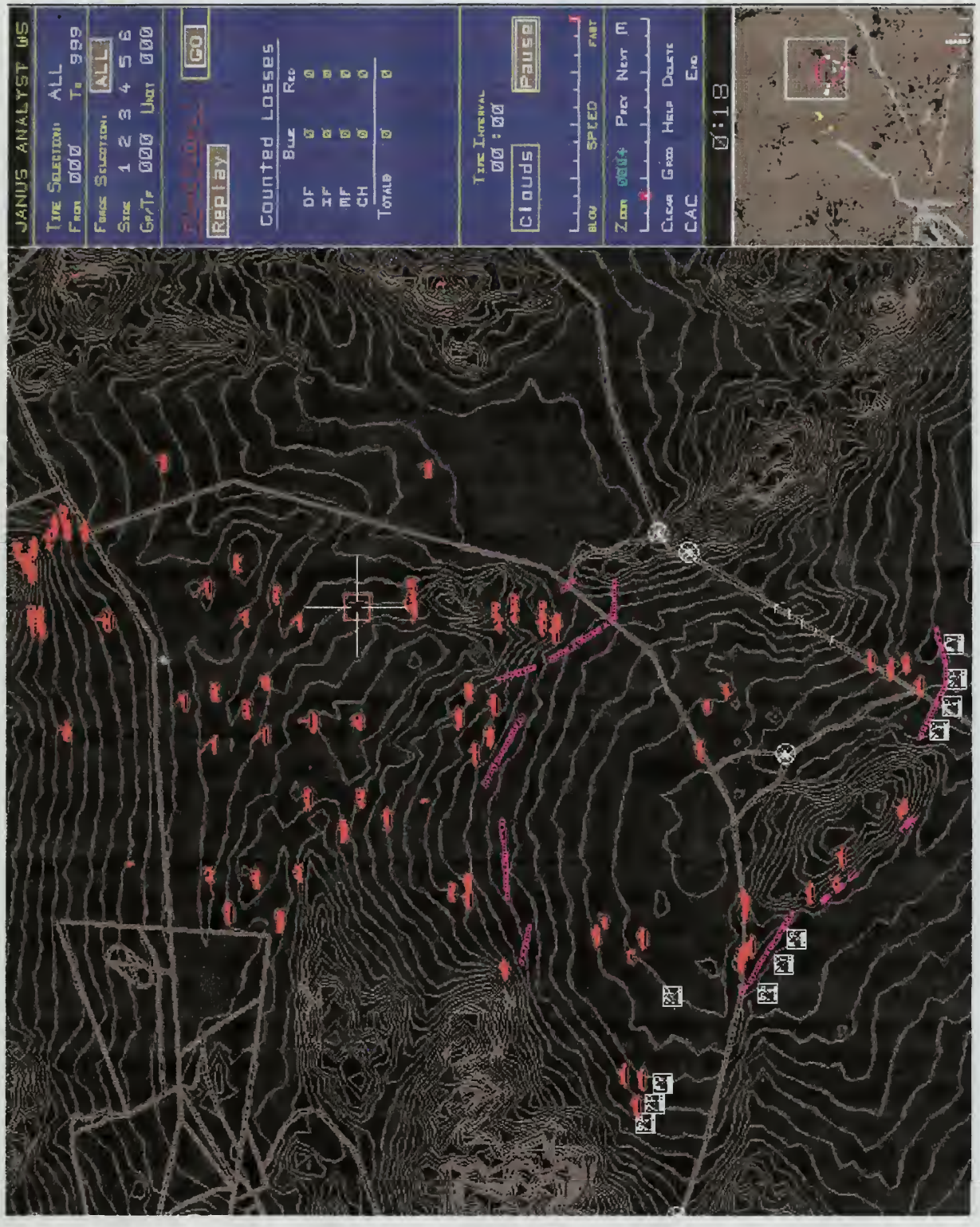


Figure 2. REDFOR Initial Disposition for AOAC 97-3 Janus Simulation

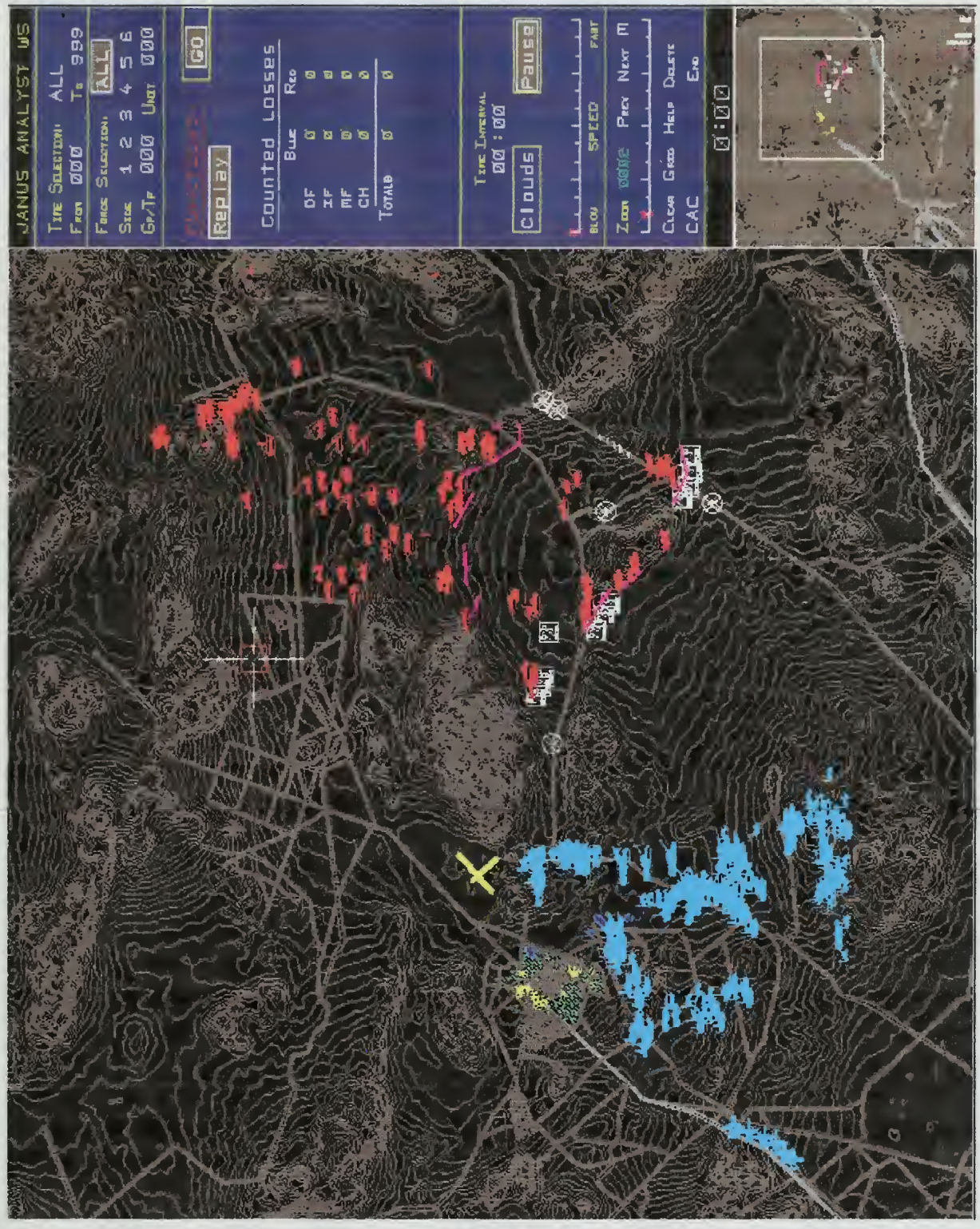


Figure 3. Battlefield Picture at Start (0 Minutes) for AOAC 97-3 Janus Simulation

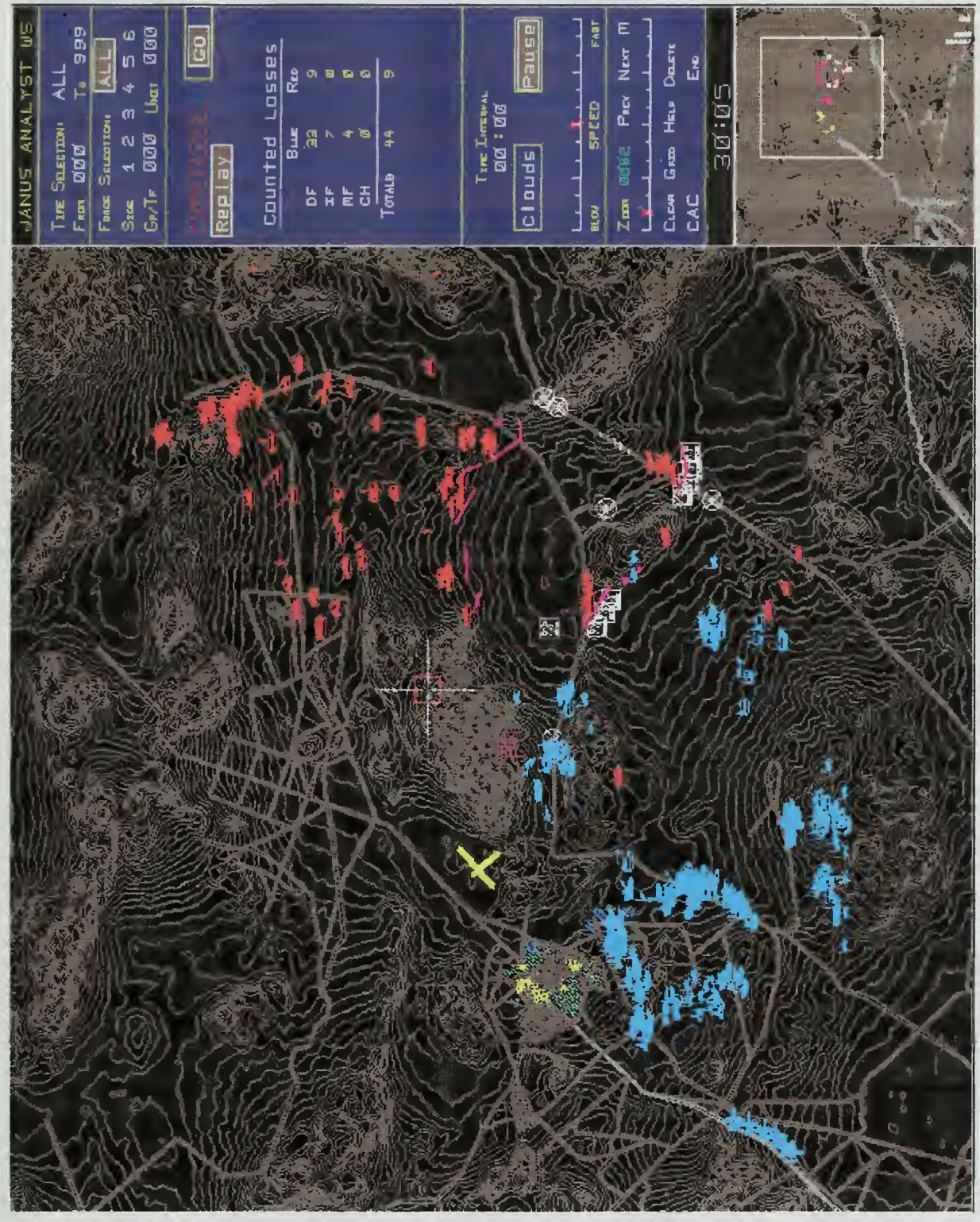


Figure 4. Battlefield Picture at 30 Minutes for AOAC 97-3 Janus Simulation

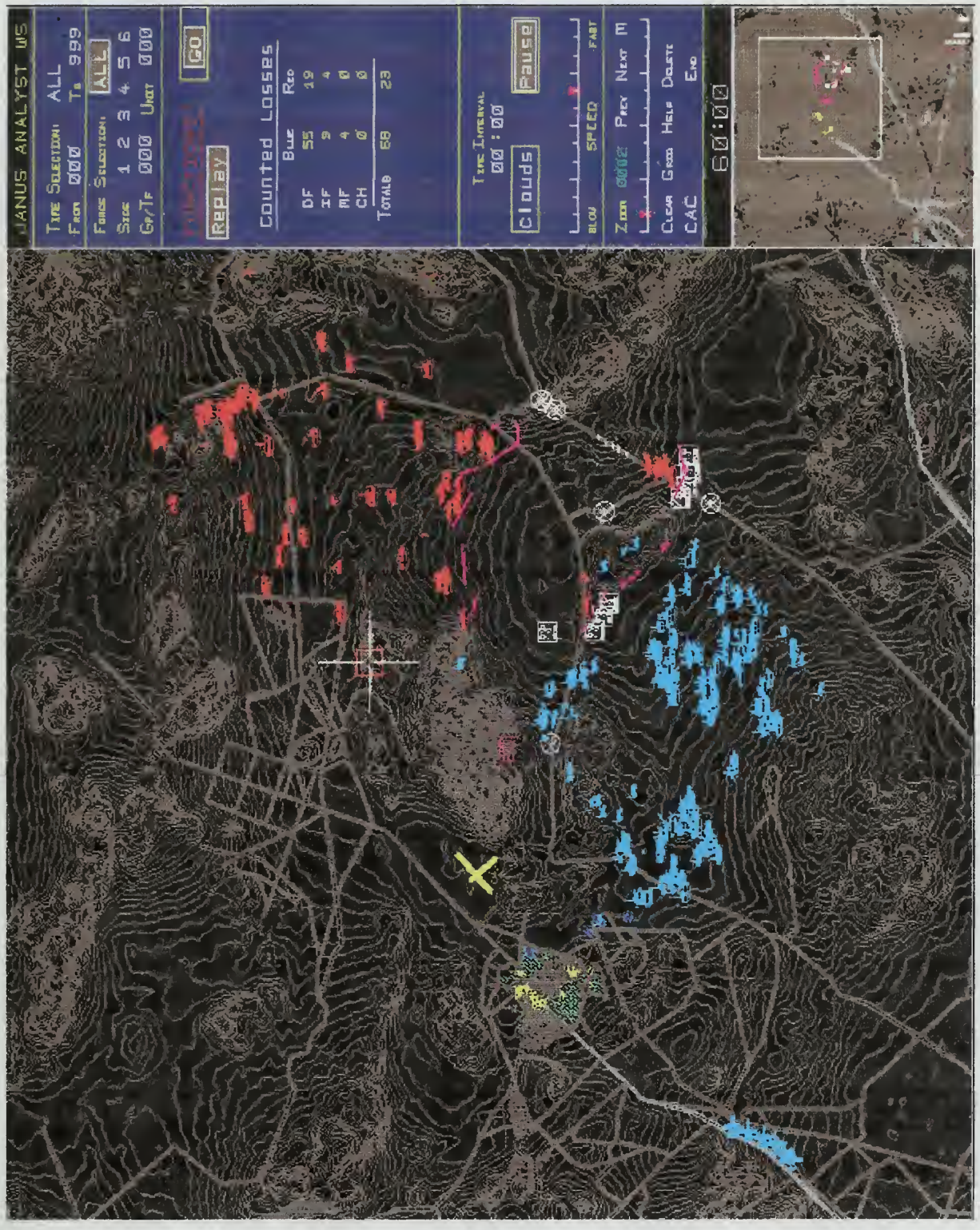


Figure 5. Battlefield Picture at 60 Minutes for AOAC 97-3 Janus Simulation

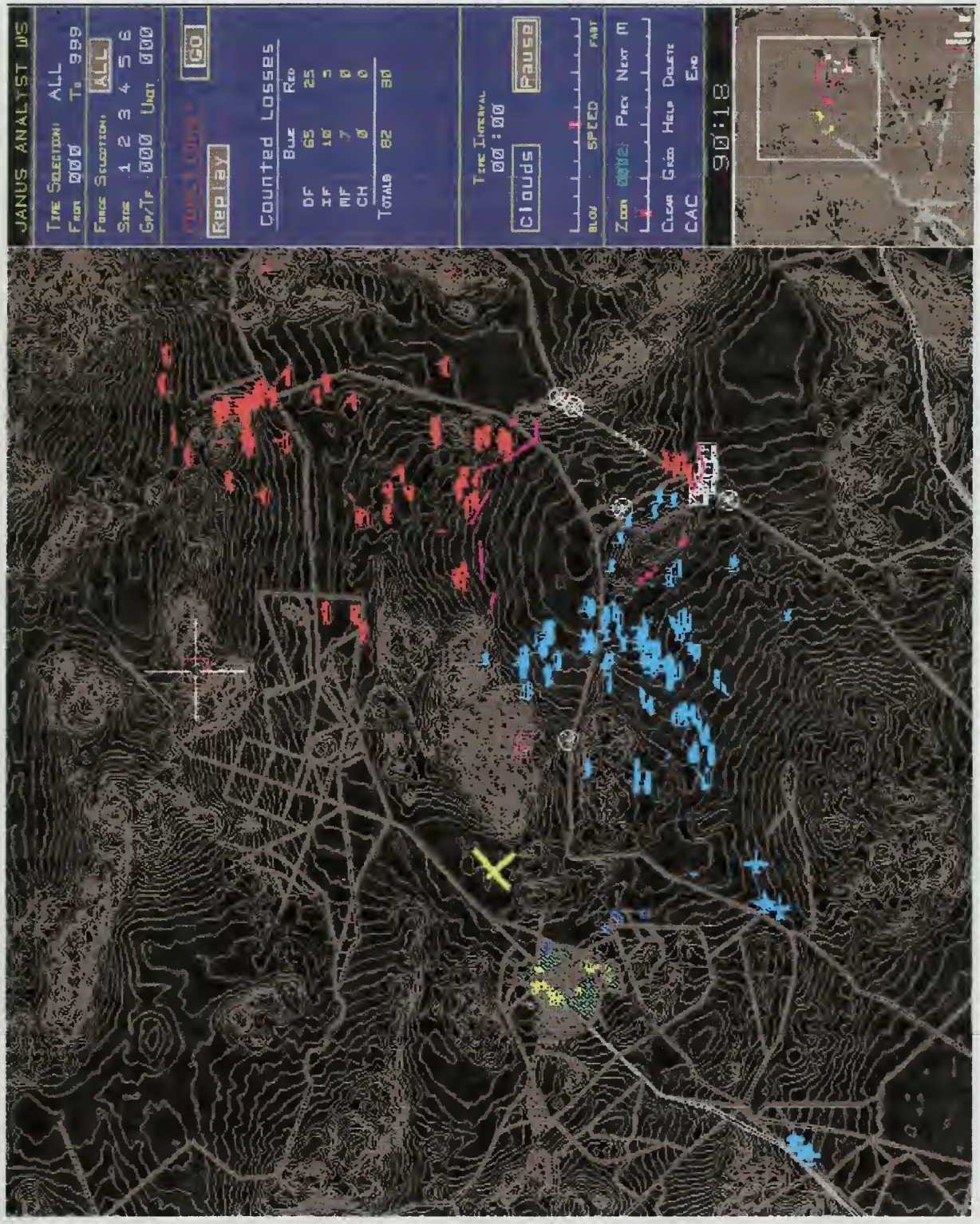


Figure 6. Battlefield Picture at 90 Minutes for AOAC 97-3 Janus Simulation

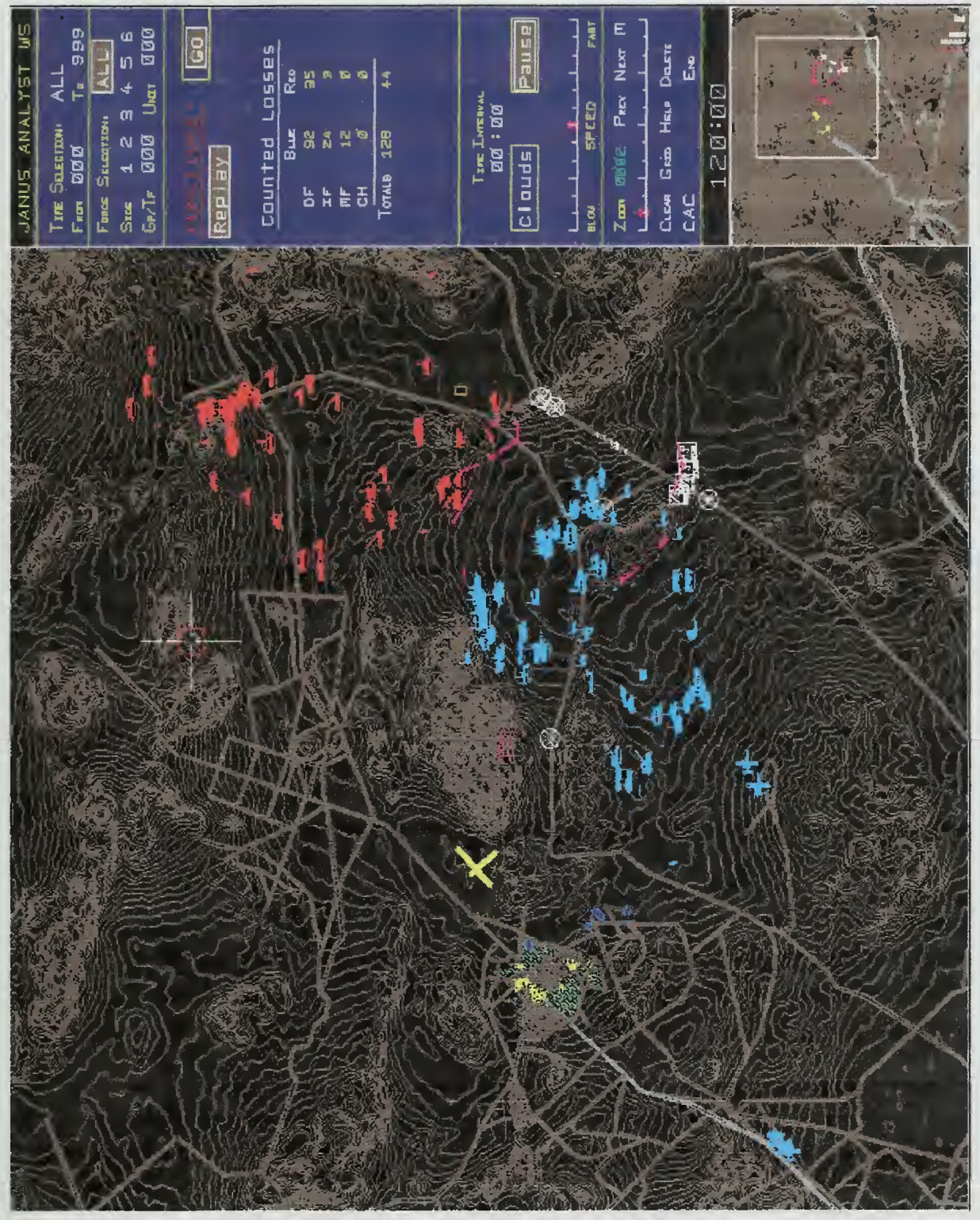


Figure 7. Battlefield Picture at 120 Minutes for AOAC 97-3 Janus Simulation

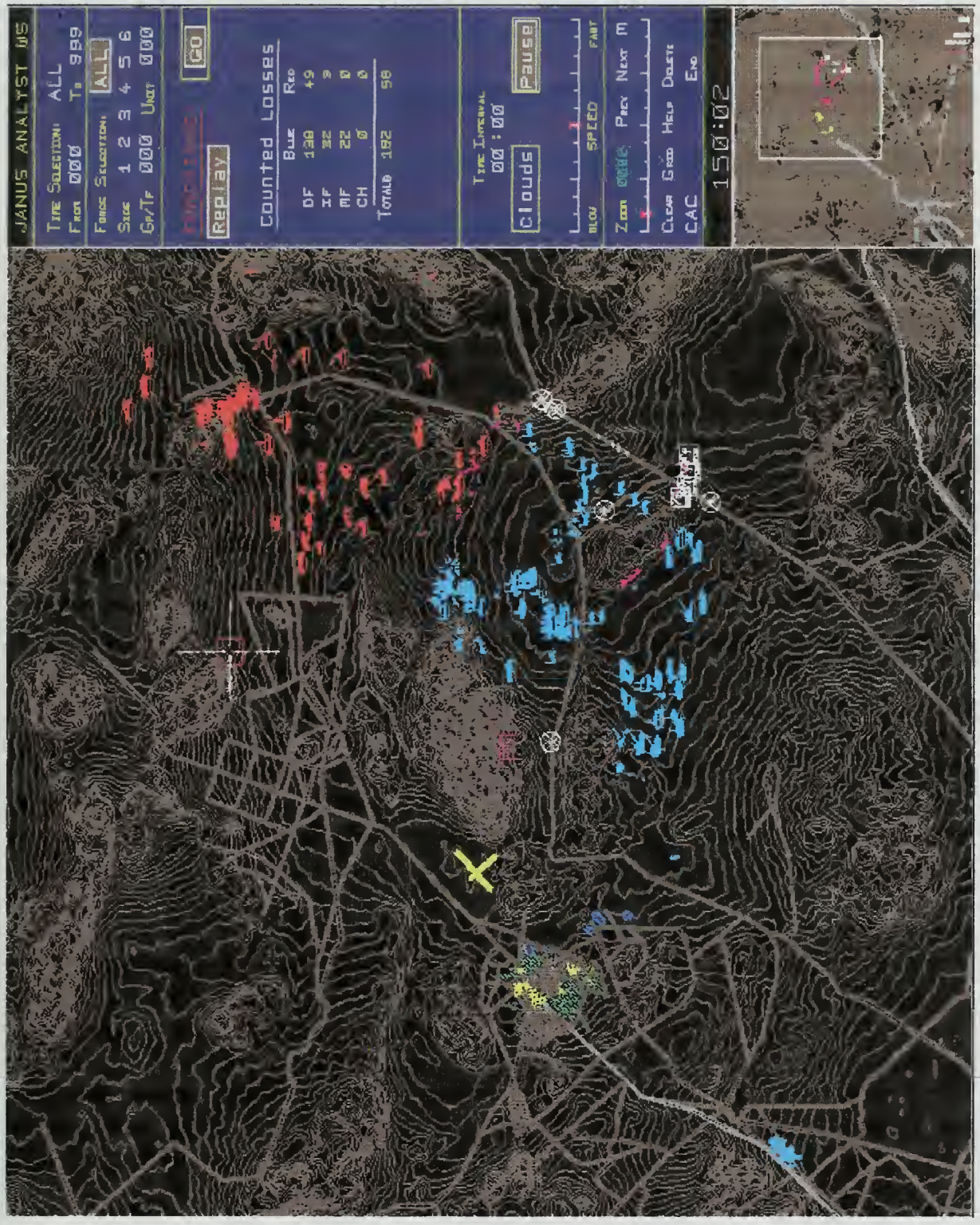


Figure 8. Battlefield Picture at 150 Minutes for AOAC 97-3 Janus Simulation

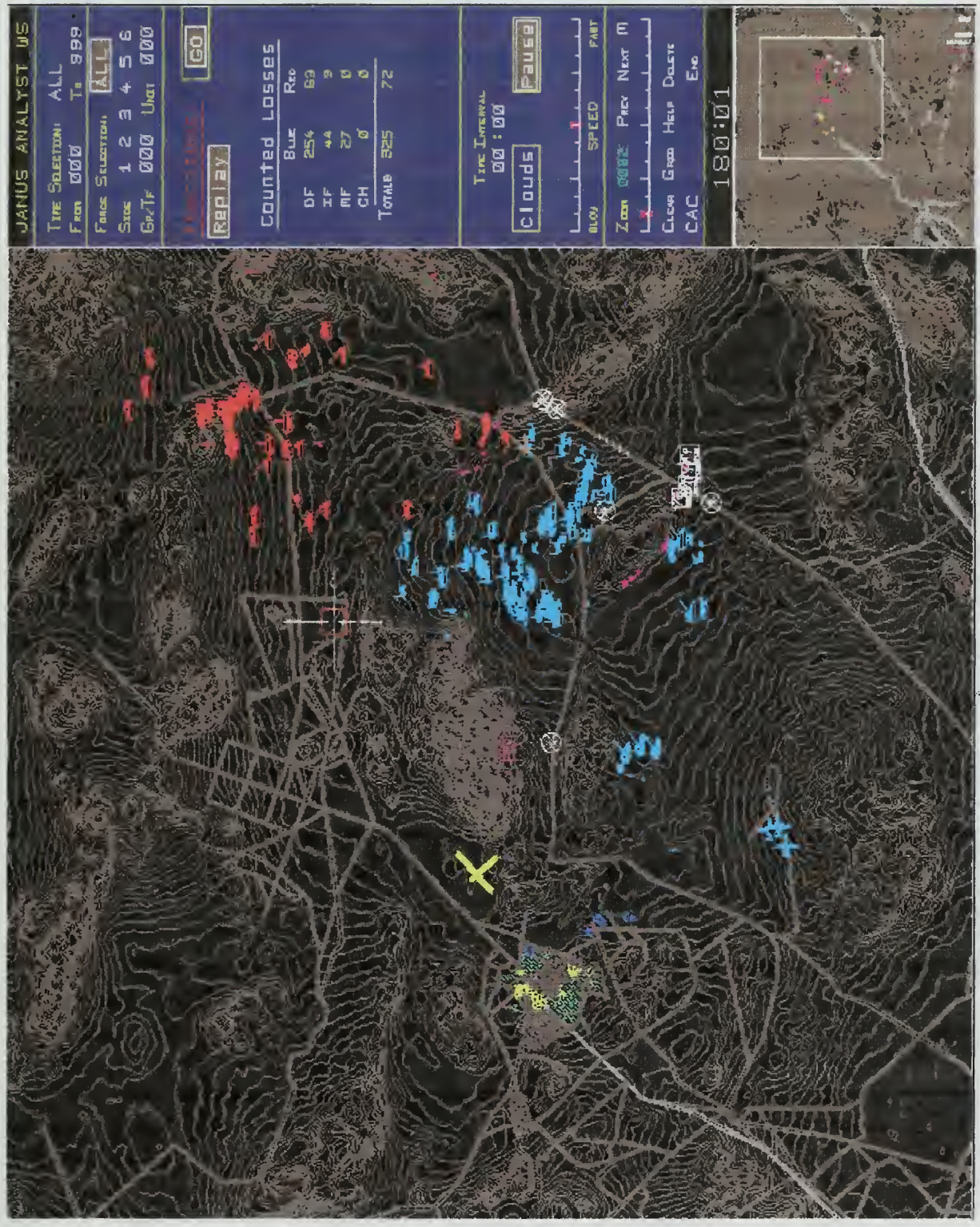


Figure 9. Battlefield Picture at 180 Minutes for AOAC 97-3 Janus Simulation

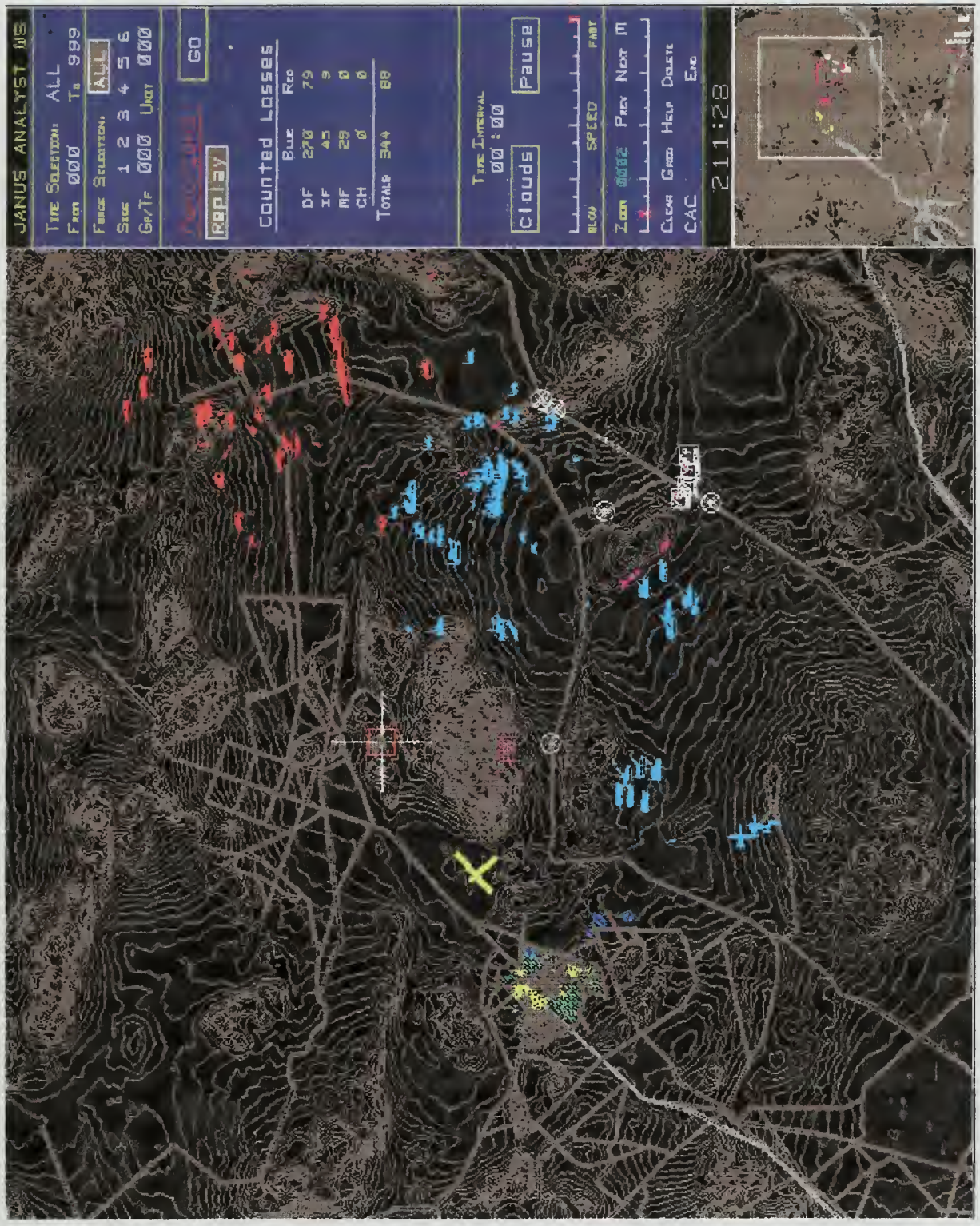


Figure 10. Battlefield Picture at Completion (211 Minutes) for AOAC 97-3 Janus Simulation

# APPENDIX B. APPLICATION OF THE ANDERSON FR METHOD TO A HYPOTHETICAL HETEROGENEOUS BATTLE REPRESENTATIVE OF THE AOAC 97-3 JANUS SIMULATION

This appendix provides the reader with an example application of the Anderson FR Method with subordinate APP process for attrition rate estimation using hypothetical kill rate data representative of the simulation output of the AOAC 97-3 Janus Simulation described in Chapter II. Specifically, the author has selectively chosen to calculate the BLUEFOR and REDFOR Firepower Scores (FPS) and the resultant Firepower Index (FPI) using two unique BLUEFOR weapon systems and three unique REDFOR weapon systems. The heterogeneous aimed fire battle between these opposing weapons systems provides the reader with a numerically obvious closed form representation for both forces' FPS.

## 1. FORCES COMPOSITION AND NOTATIONAL TRANSLATION

Let $X$ represent the BLUEFOR composed of two weapon system types, namely, 114 M1 Main Battle Tanks and 113 M2 Bradley Fighting Vehicles. Let $Y$ represent the REDFOR composed of three weapon system types, namely, 15 T-80 Main Battle Tanks, 55 BMP-2 Armored Personnel Carriers, and 17 BRDM Armored Personnel Carriers. Recall from Chapter III that the goal of the Anderson FR Method is the representation of the heterogeneous force as a single scalar measure of combat power. Translating Equation III.1 from Chapter III, we have the mathematical expressions detailed below by Equations B.1 and B.2.

$$\text{FPI}_X = \sum_{i=1}^{2} S_i^X X_i \qquad \text{(BLUEFOR Firepower Score)} \tag{B.1}$$

$i$ = integer index where 1 =M1 and 2 =M2

$S_1^X$ = value (score) of one M1

$S_2^X$ = value (score) of one M2

$X_1$ = 114 M1s

$X_2$ = 113 M2s

$$\text{FPI}_Y = \sum_{j=1}^{3} S_j^Y Y_j \qquad \text{(REDFOR Firepower Score)} \tag{B.2}$$

$j$ = integer index where 1 =T-80, 2 =BMP-2, and 3 =BRDM

$S_1^Y$ = value (score) of one T-80

$S_2^Y$ = value (score) of one BMP-2

$S_3^Y$ = value (score) of one BRDM

$Y_1$ = 15 T-80s

$Y_2$ = 55 BMP-2s

$Y_3$ = 17 BRDMs

## 2. DETERMINATION OF WEAPON SYSTEM VALUES

Recall that the fundamental methods for determining the values of $S_i^X$ and $S_j^Y$ include the analysts' perception of combat value, historical combat performance, measures of weapon firepower and support platform characteristics, and, measures of what a weapon can kill. The last method attempts to compute the value (score) for a weapon as being proportional to the rate at which it destroys the value of opposing enemy systems. This method for determining weapons system scores, called the AntiPotential-Potential (APP) method, is the primary focus of this appendix.

The formulation of the APP problem relies upon the "rate" at which systems destroy opposing systems in battle. These assumed or derived non-negative scalar attrition rates (one for each weapon system firing at every opposing weapon system for both forces) account for the highly detailed engagement process described in Chapter I. While the actual kill rates for each pairwise combination of weapon systems resulting from the Janus simulation described in Chapter II could be derived through analyzing the killer/victim scoreboard, the author has chosen to use hypothetical kill rate values for each pair of interacting weapon systems thus defining kill rate matrices, $K_{ij}$ and $L_{ji}$ below. This simplification assists the reader with focussing on the task at hand, understanding the Anderson FR methodology and the subordinate APP process. An example derivation of attrition rates from high resolution output is discussed in detail in Appendix C.

$$K_{ij} = \begin{bmatrix} .4 & .5 & .5 \\ .2 & .3 & .4 \end{bmatrix} \qquad \text{and} \qquad L_{ji} = \begin{bmatrix} .4 & .5 \\ .3 & .4 \\ .2 & .3 \end{bmatrix}$$

The matrix $K_{ij}$ represents the rate at which one type $i$ weapon system (1=M1 and 2=M2) kills type $j$ weapon systems (1=T-80, 2=BMP-2, and 3=BRDM). Analogously, $L_{ji}$ represents the rate at which one type $j$ weapon system kills type $i$ weapon systems. As an illustration, the reader will note that the BLUEFOR ($X$ force) M1 Main Battle Tank kills the REDFOR ($Y$ force) BMP-2 Armored Personnel Carrier at the rate of $K_{12} = .5$.

The remaining unknowns of Equations B.1 and B.2 are the weapon systems scores, $S_i^X$ and $S_j^Y$. Deriving these individual scores equates to solving Equations B.3 and B.4 (below) for the unknowns $C_X, C_Y, S_i^X$, and $S_j^Y$.

$$C_X S_i^X = \sum_{j=1}^{3} K_{ij} S_j^Y \qquad \text{for } i = 1, 2 \tag{B.3}$$

$$C_Y S_j^Y = \sum_{i=1}^{2} L_{ji} S_i^X \qquad \text{for } j = 1, 2, 3 \tag{B.4}$$

$$C_X = \text{proportionality constant}$$

$$C_Y = \text{proportionality constant}$$

So, for example, the value of the BLUEFOR M1 Main Battle Tank ($S_1^X$) is proportional to ($C_X$) the sum total value of every REDFOR system that it kills. The reader will note that the first equation above represents two equations (one each for $i = 1, 2$) and the second equation represents three equations (one each for $j = 1, 2, 3$) for a total of five equations. Moreover, this system of five equations has seven unknown variables, $C_X, C_Y, S_1^X, S_2^X, S_1^Y, S_2^Y$, and $S_3^Y$. A system of linear equations with more unknowns than equations defining them is referred to as underdetermined.

### a. Developing the Representative Eigenvalue Problem

To solve the value equations defined by Equations B.3 and B.4, consider the following substitutions.

$$\begin{aligned} C_Y S_j^Y &= \sum_{i=1}^{2} L_{ji} S_i^X \qquad \text{for } j = 1, 2, 3 \\ \Longleftrightarrow S_j^Y &= \frac{1}{C_Y}\left(\sum_{i=1}^{2} L_{ji} S_i^X\right) \qquad \text{for } j = 1, 2, 3 \end{aligned}$$

Substituting the expression for $S_j^Y$ above into Equation B.3 yields

$$\begin{aligned} C_X S_i^X &= \sum_{j=1}^{3} K_{ij}\left[\frac{1}{C_Y}\left(\sum_{i=1}^{2} L_{ji} S_i^X\right)\right] \qquad \text{for } i = 1, 2 \\ \Longleftrightarrow C_X C_Y S_i^X &= \sum_{i=1}^{2}\sum_{j=1}^{3}\left(K_{ij} L_{ji} S_i^X\right) \qquad \text{for } i = 1, 2\ , \end{aligned} \tag{B.5}$$

and, applying the same construct to Equation B.4

$$C_X C_Y S_j^Y = \sum_{j=1}^{3}\sum_{i=1}^{2}\left(L_{ji} K_{ij} S_j^Y\right) \qquad \text{for } j = 1, 2, 3\ . \tag{B.6}$$

For clarity, Equations B.5 and B.6 can be expressed more compactly using vector and matrix notation as depicted by Equations B.7 and B.8. Note that $\sum_{i=1}^{2}\sum_{j=1}^{3}(K_{ij}L_{ji}) = (KL)$ is a square matrix of dimension (2x2) and $\sum_{j=1}^{3}\sum_{i=1}^{2}(L_{ji}K_{ij}) = (LK)$ is a square matrix of dimension (3x3).

$$KL = \begin{bmatrix} .4100 & .5500 \\ .2500 & .3400 \end{bmatrix} \qquad \text{and} \qquad LK = \begin{bmatrix} .2600 & .3500 & .4000 \\ .2000 & .2700 & .3100 \\ .1400 & .1900 & .2200 \end{bmatrix}$$

$$C_X C_Y \vec{S}^X = (KL)\vec{S}^X \tag{B.7}$$

$$C_X C_Y \vec{S}^Y = (LK)\vec{S}^Y \tag{B.8}$$

By letting $\lambda = C_X C_Y$ [Ref. 9], the reader will note that Equations B.7 and B.8 can be written as depicted below and represent a pair of eigenvalue problems which will share common eigenvalues.

$$\lambda\vec{S}^X = (KL)\vec{S}^X \tag{B.9}$$

$$\lambda\vec{S}^Y = (LK)\vec{S}^Y \tag{B.10}$$

The reader should note that the matrix products $(KL)$ and $(LK)$ are square matrices which have only positive entries. Consequently, the *Perron-Frobenius Theorem* states that the largest eigenvalue of a matrix with only positive entries and the entries of the eigenvector associated with the largest eigenvalue are positive real numbers. See [Ref. 12].

## b. Solving the Representative Eigenvalue Problem

The eigenvalue problems represented by Equations B.9 and B.10 can be solved by finding the roots of the respective characteristic equations,

$$det(KL - \lambda I) = 0$$

$$\Longleftrightarrow det(\begin{bmatrix} .4100-\lambda & .5500 \\ .2500 & .3400-\lambda \end{bmatrix}) = 0 \tag{B.11}$$

and,

$$\begin{aligned} det(LK-\lambda I) &= 0 \\ \Longleftrightarrow det(\begin{bmatrix} .2600-\lambda & .3500 & .4000 \\ .2000 & .2700-\lambda & .3100 \\ .1400 & .1900 & .2200-\lambda \end{bmatrix}) &= 0 \end{aligned}$$

where *det* is defined as the determinant and $I$ is the identity matrix of the appropriate dimension. These characteristic equations are simplified to the following equations by evaluating the determinant and collecting like terms. If required, the reader can review the methods for evaluating determinants of (2x2) and (3x3) matrices in [Ref. 12].

$$\begin{aligned} det(KL-\lambda I) &= (.4100-\lambda)(.3400-\lambda)-(.2500)(.5500) \\ &= \lambda^2-.7500\lambda+.0019 \end{aligned}$$

and

$$\begin{aligned} det(LK-\lambda I) &= (.2600-\lambda)[(.2700-\lambda)(.2200-\lambda)-(.1900)(.3100)] \\ &\quad -.3500[(.2000)(.2200-\lambda)-(.1400)(.3100)] \\ &\quad +.4000[(.2000)(.1900)-(.1400)(.2700-\lambda)] \\ &= -\lambda^3+.7500\lambda^2-.0019\lambda \\ &= -\lambda(\lambda^2-.7500\lambda+.0019) \end{aligned}$$

Setting both determinants equal to zero and solving for the values of $\lambda$ which fulfill these equalities (using the quadratic formula [Ref. 12]), we find that the first

characteristic equation yields roots $\lambda_1 = .7475$ and $\lambda_2 = .0025$, and, the second equation yields $\lambda_1 = .7475, \lambda_2 = .0025$, and $\lambda_3 = 0$. The reader is now able to confirm the existence of the largest eigenvalue, $\lambda^* = .7475$, which is both real and positive as ensured by the *Perron-Frobenius Theroem.* Substituting this value, $\lambda^* = .7475$, into Equations B.9 and B.10 presents the following eigenvector problems for which we seek the solutions.

$$(KL - \lambda^* I)\vec{S}^X = \vec{0} \tag{B.12}$$

$$(LK - \lambda^* I)\vec{S}^Y = \vec{0} \tag{B.13}$$

Consider Equation B.12 in isolation.

$$(KL - \lambda^* I)\vec{S}^X = \vec{0}$$

$$\iff \begin{bmatrix} -.3375 & .5500 \\ .2500 & -.4075 \end{bmatrix} \begin{bmatrix} S_1^X \\ S_2^X \end{bmatrix} = \begin{bmatrix} 0 \\ 0 \end{bmatrix}$$

As there are infinitely many eigenvectors which solve this equality, the author will arbitrarily fix $S_1^X = 1$ to produce a unique value for $S_2^X$ (and hence, a unique eigenvector). This amounts to normalizing the value of the BLUEFOR M1 Main Battle Tank equal to one, which will force all of the weapon systems values to be *scaled* relative to the M1. The reader should be aware that this scaling method is only one from a list of many methods. Further information can be found in [Ref. 9]. Solving for the second unknown (the value of the BLUEFOR M2 Bradley Fighting Vehicle), the reader can confirm that $S_2^X = .6134$. Therefore, $\vec{S}^X = \begin{bmatrix} 1 \\ .6134 \end{bmatrix}$.

However, the reader should be aware of the fact that this solution vector is not unique. Any scalar multiple of this value vector will also satisfy Equation B.12. The proportionality constants, $C_X$ and $C_Y$, appearing in Equations B.7 and B.8 will simply adjust to absorb the scalar multiple changes to the eigenvector of weapon system values - a condition for which the chosen scaling method shortly corrects.

Now consider the effectiveness of the BLUEFOR M1 Main Battle Tanks as they destroy the "value" of the REDFOR weapon systems. This can be evaluated mathematically by the expression $\sum_{j=1}^{3} K_{1j} S_j^Y$. The IDAGAM scaling method [Ref. 9] seeks to scale the values of $S_j^Y$ such that $\sum_{j=1}^{3} K_{1j} S_j^Y = \sqrt{\lambda^*}$, where $\lambda^* = .7475$ (the largest eigenvalue). Recall that in the development of the eigenvalue problems represented by Equations B.9 and B.10 that the author let $\lambda = C_X C_Y$. Combining Equation B.3 with the known information $S_1^X = 1$ and $\sum_{j=1}^{3} K_{1j} S_j^Y = \sqrt{\lambda^*}$ the reader will notice the following result.

$$\begin{aligned} C_X S_1^X &= \sum_{j=1}^{3} K_{1j} S_j^Y \\ C_X &= \sqrt{\lambda^*} \\ C_X &= \sqrt{C_X C_Y} \\ (C_X)^2 &= C_X C_Y \\ C_X &= C_Y = \sqrt{\lambda^*} \end{aligned}$$

Substituting the kill rate information from matrix $K$ into the equation $\sum_{j=1}^{3} K_{1j} S_j^Y = \sqrt{\lambda^*}$ results in the equation $.4S_1^Y + .5S_2^Y + .5S_3^Y = .8646$. This particular scaling method now calls for the replacement the first equation of the linear system represented by Equation B.13 with this new equation. This action results in the following matrix equation.

$$\begin{aligned} (LK - \lambda^* I)\vec{S}^Y &= \vec{0} \\ \iff \begin{bmatrix} .4000 & .5000 & .5000 \\ .2000 & -.4775 & .3100 \\ .1400 & .1900 & -.5275 \end{bmatrix} \begin{bmatrix} S_1^Y \\ S_2^Y \\ S_3^Y \end{bmatrix} &= \begin{bmatrix} .8646 \\ 0 \\ 0 \end{bmatrix} \end{aligned}$$

Several methods exist for solving this system of three linear equations in three unknowns (many of which are detailed in [Ref. 12] and [Ref. 13]). When solved, the resulting values for the REDFOR weapon systems are $\vec{S}^Y = \begin{bmatrix} .8176 \\ .6309 \\ .4442 \end{bmatrix}$.

## 3. CALCULATING THE RESULTANT FIREPOWER INDICES

Armed with the values for each of the BLUEFOR and REDFOR distinct weapon systems, the reader can easily calculate the single-valued scalar descriptors $\text{FPI}_X$ and $\text{FPI}_Y$.

$$\begin{aligned} \text{FPI}_X &= \sum_{i=1}^{2} S_i^X X_i \\ &= (1)(114) + (.6134)(113) \\ &= 183.3142 \end{aligned}$$

$$\begin{aligned} \text{FPI}_Y &= \sum_{j=1}^{3} S_j^Y Y_j \\ &= (.8176)(15) + (.6309)(55) + (.4442)(17) \\ &= 54.5151 \end{aligned}$$

As described in Chapter III, the Force Ratio ($\text{FR}_{XY}$) can be calculated as $\text{FR}_{XY} = \frac{\text{FPI}_X}{\text{FPI}_Y} = \frac{183.3142}{54.5151} = 3.3626$. In a simplified sense, this resultant $\text{FR}_{XY}$ would determine the outcome of a battle with respect to parameters set within an aggregated model. For a more detailed treatment of the theoretical foundations of the Anderson (FR) Method and a critique of its use in force-ratio-based attrition models, see [Ref. 9].

The reader may have gathered that the complexity associated with heterogeneous battles made up of many distinct weapon systems would require the intro-

duction of an automated capability to solve the representative eigenvalue problems. For example, thoroughly accounting for the 33 BLUEFOR and 18 REDFOR distinct weapon systems modeled in the Janus simulation described in Chapter II would result in a linear system of 51 equations in 53 unknowns (counting $C_X$ and $C_Y$). The reader may also surmise that the kill rate matrices associated with this complex simulation may be sparse; in other words, many of the entries of the kill rate matrices could be equivalent to zero based upon weapon systems which do not directly interact on the battlefield. This fact introduces another consideration to the Anderson FR method and the subordinate APP process — the possibility for ill-conditioned matrices (see [Ref. 12]). At this point, the reader should have a basic understanding of the Anderson (FR) based attrition model and its application to a simplified heterogeneous battle.

# APPENDIX C. APPLICATION OF THE COMAN MAXIMUM LIKELIHOOD ESTIMATION METHOD TO A HOMOGENEOUS BATTLE WITHIN THE AOAC 97-3 JANUS SIMULATION

This appendix provides the reader with an example application of the COMAN MLE method for attrition rate estimation using portions of the simulation output data from the AOAC 97-3 Janus Simulation described in Chapter II. Specifically, the author has chosen to apply this method to the time series of attrition between two opposing mechanized infantry weapon systems. The aimed fire battle between the BLUEFOR M2 Bradley Fighting Vehicles and the REDFOR BMP-2 Armored Personnel Carriers is examined as a homogeneous exchange of direct fires. The primary weapon systems engaged in this battle are the TOW anti-tank missile (BLUEFOR) and the AT-5 anti-tank missile (REDFOR). As such the derived attrition rate parameters will be applicable to the Lanchester Square Law (F|F) for aimed fire warfare. Finally, the author develops a practical application of the differential equations (Equations C.1 and C.2 detailed below) to validate the derived attrition rate estimates. This replay is analogous to the replay executed within the ATCAL Phase II algorithm. (However, the reader should recall that ATCAL Phase I uses an *ad hoc* method for attrition rate estimation rather than the COMAN MLE method.) The data for this analysis was exported from the Janus simulation output file and manipulated in a commercial spreadsheet software package (not included in this Appendix). The data appears in Table XIV on page 104 of this Appendix. However, the interested reader can obtain copies of the associated spreadsheet files from Professor Bard K. Mansager, Department of Mathematics, Naval Postgraduate School.

# 1. NOTATION

Let $X$ represent the BLUEFOR M2 systems (with TOW missiles) and $Y$ the REDFOR BMP-2 systems (with AT-5 missiles). The relative Lanchester Square Law equations, modified with the COMAN MLE attrition rate estimates, model the change in force size with respect to time. These are Equations C.1 and C.2.

$$\frac{dx}{dt} = -\hat{a}y(t) \qquad \text{with } x(0) = x_0 \tag{C.1}$$

$$\frac{dy}{dt} = -\hat{b}x(t) \qquad \text{with } y(0) = y_0 \tag{C.2}$$

$x(t)$ = size of force $X$ at time $t$

$y(t)$ = size of force $Y$ at time $t$

$\hat{a}$ = derived attrition rate at which BMP-2 firers kill M2 targets

$\hat{b}$ = derived attrition rate at which M2 firers kill BMP-2 targets

Recall Equations III.21 and III.22 on page 44 of Chapter III, as shown below.

$$\hat{a} = \frac{c_T^X}{\sum_{k=1}^{K} n_{k-1}(t_k - t_{k-1})}$$

$$\hat{b} = \frac{c_T^Y}{\sum_{k=1}^{K} m_{k-1}(t_k - t_{k-1})}$$

# 2. DEVELOPMENT OF THE ATTRITION RATE ESTIMATES

Applying Equations III.21 and III.22 to the Janus output data found in Table XIV, we have the following:

$$\hat{a} = \frac{c_T^X}{\sum_{k=1}^{K} n_{k-1}(t_k - t_{k-1})}$$

$$= \frac{\text{Total No. of M2 Casualties } (K)}{\sum_{k=1}^{K}(\text{No. of BMP-2 Surviving at } t_k - 1) \cdot (\text{Time between } k_{th} \text{ and } k - 1_{st} \text{ Casualty})}$$

$$= \frac{17}{469493 \text{ seconds}}$$

$$= 0.00217256 \text{ M2 kills per BMP-2 firer per minute; and,}$$

$$\hat{b} = \frac{c_T^Y}{\sum_{k=1}^{K} m_{k-1}(t_k - t_{k-1})}$$

$$= \frac{\text{Total No. of BMP-2 Casualties } (K)}{\sum_{k=1}^{K}(\text{No. of M2 Surviving at } t_k - 1) \cdot (\text{Time between } k_{th} \text{ and } k - 1_{st} \text{ Casualty})}$$

$$= \frac{12}{997883 \text{ seconds}}$$

$$= 0.00072153 \text{ BMP-2 kills per M2 firer per minute.}$$

Intuitively, from the standpoint of classic military operations, the resulting attrition rate estimates are logical with respect to the modeled combat scenario. The REDFOR is executing a layered defense with fortified positions and established fields of fire, while the BLUEFOR is on the attack characterized by weapon system exposure and less distinct fields of fire. Therefore, as one would expect, the REDFOR BMP-2 kills the BLUEFOR M2 at a higher rate than vice versa (all else being equal). This provides the analyst with a common sense oriented way of justifying his or her intermediate results.

## 3. DERIVATION OF FORCE LEVEL EQUATIONS FROM LANCHESTER'S SQUARE LAW (F|F) EQUATIONS

From Equations C.1 and C.2, the informed reader may see that these ordinary differential equations can be solved to obtain expressions for force levels as a function of time. Consider the following differential equations:

$$\begin{aligned} \frac{dx}{dt} &= -\hat{a}y(t) \\ \frac{dy}{dt} &= -\hat{b}x(t) \end{aligned}$$

which, when differentiated with respect to the independent time variable $t$, yield

$$\begin{aligned} \frac{d^2x}{dt^2} &= -\hat{a}\frac{dy}{dt} \\ \frac{d^2y}{dt^2} &= -\hat{b}\frac{dx}{dt}. \end{aligned}$$

Substituting the values for $\frac{dy}{dt}$ and $\frac{dx}{dt}$ and using the initial conditions associated with Equations C.1 and C.2, one has the following two (second order, linear, constant coefficient, and homogeneous) ordinary differential equations (ODE). For a more detailed explanation of ODEs of this type, consult [Ref. 13].

$$\begin{aligned} \frac{d^2x}{dt^2} &= \hat{a}\hat{b}x(t) && && \text{(C.3)} \\ x(0) &= x_0 && \text{initial condition 1} \\ \frac{dx(0)}{dt} &= -\hat{a}y_0 && \text{initial condition 2} \end{aligned}$$

$$\begin{aligned} \frac{d^2y}{dt^2} &= \hat{b}\hat{a}y(t) && && \text{(C.4)} \\ y(0) &= y_0 && \text{initial condition 1} \\ \frac{dy(0)}{dt} &= -\hat{b}x_0 && \text{initial condition 2} \end{aligned}$$

As such, each second order ODE can be solved using a characteristic equation after assuming general exponential solutions of the form $x(t) = c_1 \exp^{r_1 t} + c_2 \exp^{r_2 t}$ and $y(t) = c_3 \exp^{r_3 t} + c_4 \exp^{r_4 t}$. Considering the second order ODE Equation C.3 and its initial conditions in isolation, suppose that $x(t) = \exp^{rt}$, where $r$ is a parameter

to be determined. Then it follows that $\frac{dx}{dt} = r\exp^{rt}$ and $\frac{d^2x}{dt^2} = r^2\exp^{rt}$. Substituting these values into Equation C.3 yields

$$\begin{aligned} r^2\exp^{rt} &= \hat{a}\hat{b}\exp^{rt} \\ (r^2 - \hat{a}\hat{b})\exp^{rt} &= 0. \end{aligned}$$

And, since $\exp^{rt} > 0$ for all values of $t$, then $(r^2 - \hat{a}\hat{b})$ must equal zero. Therefore, $r = \pm\sqrt{\hat{a}\hat{b}}$ are the roots to the characteristic equation. Note that $\hat{a}$ and $\hat{b}$ are both positive real numbers implying that $\pm\sqrt{\hat{a}\hat{b}}$ are both positive real numbers. Knowing this, the complex and repeated root cases can be eliminated [Ref. 13]. General solutions to the second order ODE (Equation C.3) can now be represented by

$$x(t) = c_1\exp^{(\sqrt{\hat{a}\hat{b}})t} + c_2\exp^{-(\sqrt{\hat{a}\hat{b}})t}.$$

Examining the initial condition 1,

$$\begin{aligned} x(0) &= x_0 \\ \Longleftrightarrow c_1 + c_2 &= x_0, \end{aligned}$$

and initial condition 2,

$$\begin{aligned} \frac{dx(0)}{dt} &= -\hat{a}y_0 \\ \Longleftrightarrow c_1\sqrt{\hat{a}\hat{b}} - c_2\sqrt{\hat{a}\hat{b}} &= -\hat{a}y_0. \end{aligned}$$

The reader will recognize that the resulting two equations representing the initial conditions applied to our general solution form a system of two linear equations in two unknowns, namely, $c_1$ and $c_2$. Solving this system of equations yields $c_1 = \frac{1}{2}\left(x_0 - \sqrt{\frac{\hat{a}}{\hat{b}}}y_0\right)$ and $c_2 = \frac{1}{2}\left(x_0 + \sqrt{\frac{\hat{a}}{\hat{b}}}y_0\right)$. Substituting these values back into

the general form of the solutions, Equations C.5 and C.6 result. (Without loss of generality, Equation C.6 follows from the work presented for Equation C.5; the interested reader is encouraged to verify the result.)

$$x(t) = \frac{1}{2}\left\{\left(x_0 - \sqrt{\frac{\hat{a}}{\hat{b}}}y_0\right)\exp^{(\sqrt{\hat{a}\hat{b}})t} + \left(x_0 + \sqrt{\frac{\hat{a}}{\hat{b}}}y_0\right)\exp^{-(\sqrt{\hat{a}\hat{b}})t}\right\} \quad \text{(C.5)}$$

$$y(t) = \frac{1}{2}\left\{\left(y_0 - \sqrt{\frac{\hat{b}}{\hat{a}}}x_0\right)\exp^{(\sqrt{\hat{a}\hat{b}})t} + \left(y_0 + \sqrt{\frac{\hat{b}}{\hat{a}}}x_0\right)\exp^{-(\sqrt{\hat{a}\hat{b}})t}\right\} \quad \text{(C.6)}$$

As an alternative to the exponential representation of the force size equations (dependent on time $t$), one can make use of the hyperbolic functions $\cosh = \frac{\exp^{\theta} + \exp^{-\theta}}{2}$ and $\sinh = \frac{\exp^{\theta} - \exp^{-\theta}}{2}$ to transform Equations C.5 and C.6 into

$$x(t) = x_0 \cosh\left[\left(\sqrt{\hat{a}\hat{b}}\right)t\right] - y_0\sqrt{\frac{\hat{a}}{\hat{b}}}\sinh\left[\left(\sqrt{\hat{a}\hat{b}}\right)t\right] \quad \text{(C.7)}$$

$$y(t) = y_0 \cosh\left[\left(\sqrt{\hat{a}\hat{b}}\right)t\right] - x_0\sqrt{\frac{\hat{b}}{\hat{a}}}\sinh\left[\left(\sqrt{\hat{a}\hat{b}}\right)t\right]. \quad \text{(C.8)}$$

The most significant advantage to this form is the insight provided for the parametric relationships that exist within the force level equations themselves. Consider the comparison of force size at time $t$ compared to the initial force size for a hypothetical force $X$. This can be accomplished by dividing Equation C.7 by $x_0$, resulting in

$$\frac{x(t)}{x_0} = \cosh\left[\left(\sqrt{\hat{a}\hat{b}}\right)t\right] - \frac{y_0}{x_0}\sqrt{\frac{\hat{a}}{\hat{b}}}\sinh\left[\left(\sqrt{\hat{a}\hat{b}}\right)t\right]. \quad \text{(C.9)}$$

From Equation C.9, the reader can see that the level of force $X$ appears to be dependent upon three terms; the initial force ratio $\left(\frac{y_0}{x_0}\right)$, the relative fire effectiveness measure $\left(\frac{\hat{a}}{\hat{b}}\right)$, and what can be called the intensity of combat indicator $\left(\sqrt{\hat{a}\hat{b}}\right)$. In a battle to annihilation, these indicator values can be used to generalize simulation results [Ref. 9].

Hence, one can now deterministically solve for force sizes, $x(t)$ and $y(t)$, for the desired time $t$ using Equations C.5 and C.6 (or Equations C.7 and C.8) and the estimated attrition rate coefficients $\hat{a}$ and $\hat{b}$. This practical extension of Lanchester's Square Law (F|F) affords the analyst a straightforward method for estimating force size throughout a battle. The force size results can also be used to verify $\hat{a}$ and $\hat{b}$ themselves by comparing the numerical values of $x(t)$ and $y(t)$ to the analogous high resolution results (force size) at various points throughout the simulation. This practical exercise is what remains to be examined in this Appendix.

## 4. COMPARISON OF JANUS SIMULATION RESULTS TO THE DETERMINISTIC LANCHESTER SQUARE LAW RESULTS

Using the values for $\hat{a}$ and $\hat{b}$ derived from the Janus simulation data output, one can form the two Lanchester Square Law (F|F) Equations C.10 and C.11 below.

$$\frac{dx}{dt} = -(0.00217256)y(t) \quad \text{with } x_0 = 113 \tag{C.10}$$

$$\frac{dy}{dt} = -(0.00072153)x(t) \quad \text{with } y_0 = 55 \tag{C.11}$$

Or, equivalently, using Equations C.5 and C.6 the force size equations can be written as

$$x(t) = \frac{1}{2}\left\{\left(113 - \sqrt{\frac{\hat{a}}{\hat{b}}}55\right)\exp^{(\sqrt{\hat{a}\hat{b}})t} + \left(113 + \sqrt{\frac{\hat{a}}{\hat{b}}}55\right)\exp^{-(\sqrt{\hat{a}\hat{b}})t}\right\} \tag{C.12}$$

$$y(t) = \frac{1}{2}\left\{\left(55 - \sqrt{\frac{\hat{b}}{\hat{a}}}113\right)\exp^{(\sqrt{\hat{a}\hat{b}})t} + \left(55 + \sqrt{\frac{\hat{b}}{\hat{a}}}113\right)\exp^{-(\sqrt{\hat{a}\hat{b}})t}\right\} \tag{C.13}$$

where

$$\hat{a} = 0.00217256$$

$$\hat{b} = 0.00072153.$$

Calculating the force size values of $x(t)$ and $y(t)$ for values of $t = (0, 15, 30, \cdots, 210)$ minutes using Equations C.12 and C.13 above, the reader will note that the deterministic approximations depicted in Table XV on page 105 of this Appendix are quite representative of the Janus simulation results. (Note: The deterministic results for $x(t)$ and $y(t)$ are shown as integer results which were derived by rounding the continuous solutions to Equations C.12 and C.13). Employing the deterministic Lanchester equations to replicate the high resolution simulation results is called "replaying" the simulation. This is the role that the ATCAL Phase II algorithm plays as part of the aggregated models it supports. In this example, the deterministic Lanchester results estimate the casualties achieved during the Janus simulation with fairly high accuracy as depicted by Figures 11 and 12 on page 106. Note that the maximum absolute error of the approximations is no greater than two weapon systems for both forces.

The small discrepancies can be attributed to several facts. First, the author arbitrarily decided to single out two opposing weapon systems from a highly integrated heterogeneous combat simulation to demonstrate the mathematics associated with the homogeneous form of Lanchester's Square Law (F|F) and the COMAN MLE attrition coefficient estimation process. The reader may have already gathered that the high resolution simulation presented in Chapter II infers the need for a heterogeneous-type attrition analysis construct; however, tractable formulations do not exist for heterogeneous Lanchester-type equations. So, in presenting the simplistic closed form solutions associated with the homogeneous problem, the reader is able to gain an appreciation for the mathematics behind attrition computations. Second, examining the casualty times listed in Table XIV, one can see that the exchanges of aimed fire between the REDFOR BMP-2 (with AT-5) and the BLUEFOR M2 (with TOW) were focused around several small battles. Each force shared losses during several distinct time periods, i.e., intervals where $[t_k - t_{k-1}]$ are small and follow each other closely. The larger values of $[t_k - t_{k-1}]$ depict periods of inactivity during the battle. Perhaps distinct COMAN MLE attrition rate estimates $\hat{a}$ and $\hat{b}$ could be derived for

several time sub-intervals representing their corresponding sub-battles. Lastly, the reader should recall that this research only utilizes one stochastic sample of the high resolution simulation. A more statistically robust analysis could have been made had the attrition rate parameters been estimated after considering the time series Markov (Poisson) attrition processes for several independent simulations.

Even with the perceived shortcomings, the reader will agree that the sampled deterministic Lanchester replay of the high resolution simulation is quite good. Additionally, through the application and understanding of this simplified example, the reader should have a thorough appreciation for the expanse of this subject matter.

| Casualty Time | Target | No. Lost | Firer | $k$ | Time Interval $t_k - t_{k-1}$ | No. of M2 $(m_{k-1})$ | No. of BMP-2 $(n_{k-1})$ |
|---|---|---|---|---|---|---|---|
| 16.41 | M2 | 1 | BMP-2 | 1 | 16:41 | 113 | 55 |
| 16.56 | BMP-2 | 1 | M2 | 2 | 0:15 | 112 | 55 |
| 17.42 | M2 | 1 | BMP-2 | 3 | 0:46 | 112 | 54 |
| 18.27 | M2 | 1 | BMP-2 | 4 | 0:45 | 111 | 54 |
| 18.28 | BMP-2 | 1 | M2 | 5 | 0:01 | 110 | 54 |
| 37.26 | M2 | 1 | BMP-2 | 6 | 18:58 | 110 | 53 |
| 37.49 | M2 | 1 | BMP-2 | 7 | 0:23 | 109 | 53 |
| 38.10 | BMP-2 | 1 | M2 | 8 | 0:21 | 108 | 53 |
| 38.11 | M2 | 1 | BMP-2 | 9 | 0:01 | 108 | 52 |
| 46.32 | M2 | 1 | BMP-2 | 10 | 8:21 | 107 | 52 |
| 49.24 | BMP-2 | 1 | M2 | 11 | 2:52 | 106 | 52 |
| 59.29 | BMP-2 | 1 | M2 | 12 | 10:05 | 106 | 51 |
| 64.14 | BMP-2 | 1 | M2 | 13 | 4:45 | 106 | 50 |
| 83.12 | M2 | 1 | BMP-2 | 14 | 18:58 | 106 | 49 |
| 84.20 | BMP-2 | 1 | M2 | 15 | 1:08 | 105 | 49 |
| 84.21 | M2 | 1 | BMP-2 | 16 | 0:01 | 105 | 48 |
| 110.58 | M2 | 1 | BMP-2 | 17 | 2:37 | 104 | 48 |
| 111.13 | M2 | 1 | BMP-2 | 18 | 0:15 | 103 | 48 |
| 131.51 | M2 | 1 | BMP-2 | 19 | 20:38 | 102 | 48 |
| 142.28 | BMP-2 | 1 | M2 | 20 | 10:37 | 101 | 48 |
| 142.30 | M2 | 1 | BMP-2 | 21 | 0:02 | 101 | 47 |
| 143.03 | BMP-2 | 1 | M2 | 22 | 0:33 | 100 | 47 |
| 143.10 | BMP-2 | 1 | M2 | 23 | 0:07 | 100 | 46 |
| 149.26 | M2 | 1 | BMP-2 | 24 | 6:16 | 100 | 45 |
| 149.30 | BMP-2 | 1 | M2 | 25 | 0:04 | 99 | 45 |
| 149.48 | M2 | 1 | BMP-2 | 26 | 0:18 | 99 | 44 |
| 153.40 | M2 | 1 | BMP-2 | 27 | 3:52 | 98 | 44 |
| 173.36 | M2 | 1 | BMP-2 | 28 | 19:56 | 97 | 44 |
| 183.35 | BMP-2 | 1 | M2 | 29 | 9:59 | 96 | 44 |

Table XIV. Janus Simulation Data: Coroner's Report [Ref. 4]

| t | Janus x(t) | Lanchester x(t) | Janus y(t) | Lanchester y(t) |
|---|---|---|---|---|
| 0 | 113 | 113 | 55 | 55 |
| 15 | 111 | 113 | 54 | 55 |
| 30 | 109 | 110 | 53 | 53 |
| 45 | 108 | 107 | 51 | 52 |
| 60 | 106 | 106 | 50 | 50 |
| 75 | 105 | 106 | 49 | 49 |
| 90 | 103 | 104 | 48 | 48 |
| 105 | 101 | 104 | 47 | 48 |
| 120 | 100 | 102 | 46 | 48 |
| 135 | 98 | 101 | 45 | 48 |
| 150 | 97 | 98 | 44 | 44 |
| 165 | 96 | 97 | 43 | 44 |
| 180 | 94 | 96 | 42 | 44 |
| 195 | 93 | 96 | 41 | 43 |
| 210 | 92 | 96 | 40 | 43 |

Table XV. Comparison of Janus Attrition Data to Lanchester-Type Replay

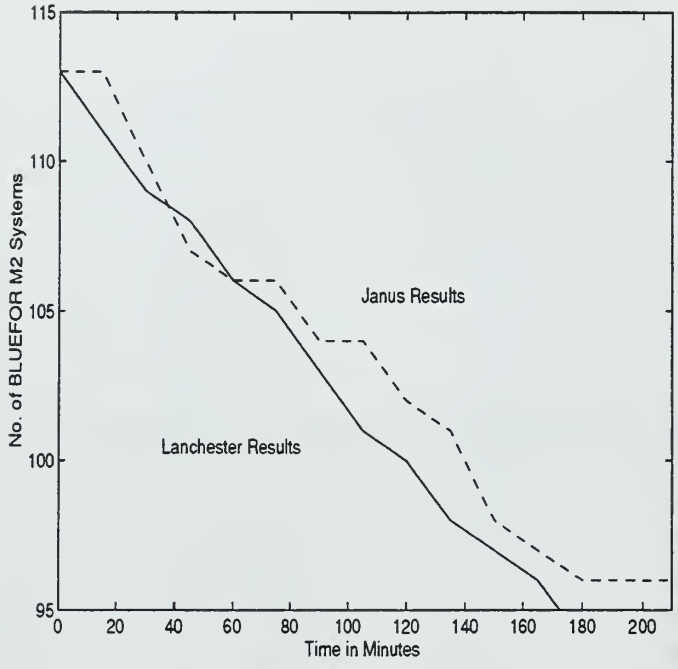


Figure 11. Graph of Force Size Over Time for BLUEFOR Simulation vs. Lanchester Replay Results

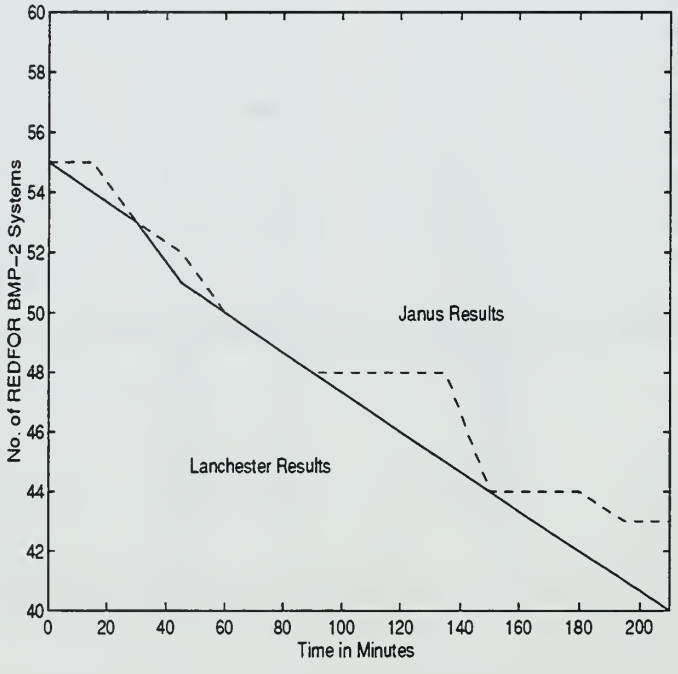


Figure 12. Graph of Force Size Over Time for REDFOR Simulation vs. Lanchester Replay Results

# INITIAL DISTRIBUTION LIST

1. Defense Technical Information Center ..... 2
   8725 John J. Kingman Rd., Ste 0944
   Ft. Belvoir, VA 22060-6218

2. Dudley Knox Library ..... 2
   Naval Postgraduate School
   411 Dyer Rd.
   Monterey, CA 93943-5101

3. U.S. Army, Concepts Analysis Agency (CAA) ..... 1
   ATTN: Edward Vandiver III and Gerry Cooper
   8120 Woodmont Ave.
   Bethesda, MD 20814

4. Office of the Deputy Undersecretary of the Army ..... 1
   SAUS-OR (Vern Bettencourt)
   102 Army Pentagon (Room 1E643)
   Washington, DC 20310-0102

5. Director, TRADOC Analysis Center ..... 1
   ATTN: ATRC (Steve Herndon)
   255 Sedgwick Ave.
   Fort Leavenworth, KS 66027-2345

6. Colonel David C. Arney ..... 1
   United States Military Academy
   Department of Mathematical Sciences
   West Point, NY 10996

7. Colonel James L. Kays ..... 1
   United States Military Academy
   Department of Systems Engineering
   West Point, NY 10996

8. Chairman Walter M. Woods, Code MA/Wo ..... 1
   Department of Mathematics
   Naval Postgraduate School
   1411 Cunningham Rd., Rm 341
   Monterey, CA 93943-5216

9. Professor Bard K. Mansager, Code MA/Ma ..... 1
   Department of Mathematics
   Naval Postgraduate School
   1411 Cunningham Rd., Rm 341
   Monterey, CA 93943-5216

10. Professor James G. Taylor, Code OA/Tw ..... 1
    Department of Operations Analysis
    Naval Postgraduate School
    1411 Cunningham Rd., Rm 257
    Monterey, CA 93943-5216

11. Professor Maurice Weir, Code MA/Wc ..... 1
    Department of Mathematics
    Naval Postgraduate School
    1411 Cunningham Rd., Rm 363
    Monterey, CA 93943-5216

12. Captain(P) Michael L. Shenk ..... 2
    United States Military Academy
    Department of Mathematical Sciences
    West Point, NY 10996